Journal of Nematology
Volume 58 Issue 1 · pp. 623–644 · DOI: 10.2478/jofnem-2026-0033

JOURNAL OF NEMATOLOGY

First report of *Helicotylenchus microlobus*, *Mesocriconema nebraskense* and *Meloidogyne naasi* from turfgrass in Utah, USA, based on comprehensive morphological, morphometric, and molecular data

Research Article

Yongsan Zeng[1], Adam Van Dyke[2], Joseph A. Roberts[1]*

[1] *Pee Dee Research and Education Center, Department of Plant and Environmental Sciences, Clemson University, 2200 Pocket Road, Florence, SC 29506, USA*
[2] *Professional Turfgrass Solutions, LLC, 2846 W Lincoln Cove, South Jordan, UT 84095, USA*

Received 26 March 2026; Accepted 27 July 2026

Abstract: The core soil samples collected from annual bluegrass at a golf course in Oakridge Country Club, Utah, USA were submitted for identification in July 2024. A high number of *Helicotylenchus* sp., *Mesocriconema* sp. females, and *Meloidogyne* sp. juveniles were recovered from the samples using the rapid centrifugal-flotation and mist chamber extraction methods. They were examined by morphological observation and morphometric measurements under light microscopy, and by analysis of sequences from multiple molecular markers, including the ribosomal DNA 18S, 28S, and ITS. Morphological characteristics and morphometrics, as well as BlastN comparisons with other population sequences of respective nematodes from GenBank, were consistent with identification as *Helicotylenchus microlobus, Mesocriconema nebraskense,* and *Meloidogyne naasi.* Phylogenetic trees inferred from rDNA18S, 28S, and ITS sequences all separated the Utah population into a strongly supported clade with other respective isolates of *H. microlobus, Mesocriconema nebraskense,* and *Meloidogyne naasi.* This study first comprehensively reports morphological and molecular characterization of *H. microlobus, Mesocriconema nebraskense* and *Meloidogyne naasi* from turfgrass in Utah, USA.

Keywords: Helicotylenchus microlobus • Mesocriconema nebraskense • Meloidogyne naasi • *Turfgrass* • *Morphology* • *18S rRNA* • *28S rRNA* • *Internal transcribed spacer (ITS)* • *Ribosomal DNA (rDNA)* • *Taxonomy* • *Phylogeny*

Turfgrass plays an important role in beautifying home lawns and setting up desirable outdoor playing surfaces for recreation and sport fields, including thousands of golf courses. However, turfgrass is often impacted by plant-parasitic nematodes (PPNs), which have become a serious problem in turfgrass management worldwide. Nematode problems emphasize the need for more understanding of nematodes infecting turfgrasses, including species identification, so that targeted and sustainable management strategies can be developed (Zeng et al., 2022). Surveys of nematodes associated with turfgrasses have been conducted and have shown a broad diversity of plant-parasitic nematodes from different countries and regions (Crow, 2005; Mwamula et al., 2021; Sánchez-Arce et al., 2021; Vandenbossche et al., 2011; Yu et al., 1998; Zeng et al., 2012a, 2012b). Fifty-two different species/taxa belonging to 23 genera and nine families in Belgium (Vandenbossche et al., 2011), nine genera in southern Ontario, Canada (Yu et al., 1998), 28 species/taxa belonging to 16 genera and 12 families in Korea (Mwamula et al., 2021); and five prevalent species (*Helicotylenchus dihystera* (Cobb), Sher, 1966, *Mesocriconema xenoplax* (Raski), Loof & De Grisse, 1989, *Meloidogyne graminis* (Sledge & Golden), Whitehead, 1968, *Hemicriconemoides rosae* Rathour, Sharma, Singh & Ganguly, 2003 and *Tylenchorhynchus leviterminalis* Siddiqi et al., 1982) in Guangdong, China (Zeng et al., 2022) were reported. In the USA, five common genera were reported in Florida (Crow, 2005), 29 species belonging to 22 genera in 15 families were reported in North Carolina and South Carolina (Zeng et al., 2012a), six genera (*Meloidogyne* spp., *Heterodera* spp., *Anguina pacificae* Cid del Prado Vera &

* *E-mail: jar7@clemson.edu*

Open Access. © 2026 the author(s), published by Society of Nematologists, Inc.
This work is licensed under the Creative Commons Attribution-NonCommercial-NoDerivs 4.0 License.

Maggenti, 1984, *Criconemella* spp. and *Trichodorus* spp.) were frequently associated with turfgrass in the western USA (McClure et al., 2012), and 11 genera (*Gracilacus, Helicotylenchus, Heterodera, Meloidogyne, Mesocriconema, Paratrichodorus, Paratylenchus, Pratylenchus, Punctodera, Rotylenchus, and Xiphinema*) were reported at golf courses on the southern coast of Oregon (Braithwate et al., 2025). Two species, *Helicotylenchus pseudorobustus* and *Meloidogyne naasi*, were the most frequently encountered PPNs on the southern coast of Oregon (Braithwate et al., 2025). Utah has about 126 golf courses; however, little on species diversity of PPNs from turfgrass has been published. Recent sampling from several golf courses in Utah showed that PPNs have impacted the growth of turfgrass and revealed the three most prevalent species. Preliminary morphological observations indicated that the population appeared to be related to *Helicotylenchus microlobus* Perry *in* Perry et al., 1959; *Mesocriconema nebraskense* Olson et al., 2017; and *Meloidogyne naasi* Franklin, 1965. Traditionally, species identification of the genera *Helicotylenchus*, *Mesocriconema,* and *Meloidogyne* relies on morphological features and morphometric characters. However, in some cases, species discrimination is much more challenging due to their phenotypic plasticity (Subbotin et al., 2011, 2015). rDNA-based approaches using the small subunit (SSU) rRNA gene, D2–D3 expansion segments of the large subunit (LSU) rRNA gene, ITS rRNA gene, and mitochondrial cytochrome c oxidase subunit I (mtCOI) have been employed to accurately identify nematode species or uncover new and cryptic species and to analyze phylogenetic relationships among species within the *Helicotylenchus* (Mwamula et al., 2024; Palomares-Rius et al., 2018; Rybarczyk-Mydłowska et al., 2019; Shokoohi et al., 2021; Subbotin et al., 2011, 2015; Zameleh et al., 2020). The objectives of this articles were to: (*i*) characterize these three species based upon integrative taxonomic approaches including morphological, morphometric, and molecular data (partial 18S rRNA and 28S rRNA sequences or ITS rRNA); and (*ii*) determine the molecular phylogenetic affinities of these three species with closely related species based on sequences of the 18S rRNA and 28S rRNA or ITS rRNA.

1. Materials and methods

1.1 Soil sampling

In July 2024, a total of eight separate composite soil samples were collected from the root zone of annual bluegrass (*Poa annua* L.) on a golf course at Oakridge Country Club, Utah, USA (41.0006° N, 111.9242° W) for extracting and analyzing nematodes. Each composite sample consisted of 12 soil cores (1.5 cm diam. × 20 cm deep) sampled at roughly equal spacing in a zig–zag pattern across an area of 500 m^2 or less. Each soil sample containing 12 soil cores was placed in a sealed plastic bag that was then placed in a sample box and stored at 4°C before analysis to minimize changes in nematode populations.

1.2 Morphological characterization

Nematodes were extracted from soil samples using the rapid centrifugal-flotation method (Jenkins, 1964). Soil samples were first suspended in water and sieved using a combination of two sieve sizes (850 µm/No. 20 on top and 38 µm/No. 400 on the bottom) to remove debris. The suspension was then centrifuged (1,500 rpm for 3 min) to concentrate heavier soil particles at the bottom of the tube. A sugar solution (907 g sugar dissolved in 2,000 mL of water) was added to the centrifuged sample, followed by a second centrifugation (1,500 rpm for 3 min). Nematodes present in the supernatant were then collected for examination. The root-knot nematode was also extracted by the mist chamber extraction method (Crow et al., 2020). In the mist chamber with a misting rail and superfine mist emitter, a 15-cm flexible rubber tubing was fitted onto the funnel (15-cm-diam. at top) stem and positioned in the funnel slot, with the tubing slightly inserted into 250-mL flask openings; then, a coffee filter was placed onto the funnels, and four turf plugs (3.8 cm in diam.) were placed in each funnel. The nematodes emerging from plant material migrated through the filter and then moved via water flow into the flask below. The mist timer was set to apply mist for 10 s each hr. After incubating for 72 hr, the nematodes were collected for identification. Specimens were heat-killed, fixed in 3% formaldehyde, and processed in glycerin using the formalin-glycerin method (Hooper, 1970). Measurements of nematodes were made using Jenoptik Gryphax® image analysis software. The morphometric data were processed using Excel software (Ye, 1996). Photomicrographs were taken using a camera (Jenoptik Gryphax®) attached to a microscope (Nikon Labophot) and edited using Adobe Photoshop CS6.

1.3 Molecular characterization

Five females (ring and spiral nematodes) or 10 juveniles (root-knot nematode) were hand-picked and placed into 50 µL of worm lysis buffer (WLB) containing Proteinase K for DNA extraction (Williams et al., 1992). DNA samples were stored at –20°C until used as a PCR template.

The primers for small subunit (SSU) 18S amplification and DNA sequencing were forward primer 18SnF (5′-TGG ATAACTGTGGTAATTCTAGAGC-3′) and reverse primer 18SnR (5′-TTACGACTTTTGCCCGGTTC-3′) (Kanzaki & Futai, 2002). Two pair of primers for large subunit (LSU) 28S amplification and DNA sequencing were forward primer 391a (5′-AGCGGAGGAAAAGAAACTAA-3′) and reverse primer 501 (5′-TCGGAAGGAACCAGCTACTA-3′ (Nadler et al., 2006), and D2A (5′-ACAAGTACCGTGAGGGAAAGT-3′), and reverse primer D3B (5′-TCGGAAGGAACCAGCTACTA-3′) (Nunn, 1992). The primers for ITS amplification and DNA sequencing were forward primer ITSUniF (5′-GTGCATGGC CGTTCTTAGTT-3′) and reverse primer Nxy22 (5′- TTCACTG CGTTCTTCATCGATC-3′) (Ye et al., 2019).

PCR (25 µL) was performed using Apex Taq RED Master Mix DNA polymerase (Genesee Scientific) according to the manufacturer's protocol. The thermal cycler program for PCR was as follows: denaturation at 95°C for 5 min, followed by 35 cycles of denaturation at 94°C for 30 s, annealing at 55°C for 45 s, and extension at 72°C for 2 min. A final extension was performed at 72°C for 10 min (Ye et al., 2007). PCR products were cleaned using ExoSap-IT (Affymetrix Inc.) according to the manufacturer's protocol. DNA sequencing was performed using PCR primers for direct sequencing by dideoxynucleotide chain termination using an ABI PRISM BigDye Terminator Cycle Sequencing Ready Reaction Kit (Applied Biosystems) in an Applied Biosystems 3730 XL DNA Analyzer (Applied Biosystems) by the Genomic Sciences Laboratory (North Carolina State University, Raleigh, NC, USA).

The rDNA SSU, LSU (391a-501, D2–D3), and ITS sequences from this project were deposited in the GenBank database under the accession numbers presented in Table 1. The DNA sequences were compared with other nematode species in GenBank using the BLAST homology search program (https://blast.ncbi.nlm.nih.gov/Blast.cgi? PROGRAM = blastn&PAGE_TYPE = BlastSearch&LINK_LOC = blasthome). The most similar sequences were downloaded for phylogenetic analysis. DNA sequences were aligned using Mega5.05 (Tamura et al., 2011). The model of base substitution in the SSU and LSU sets was evaluated using MODELTEST version 3.06 (Posada & Crandall, 1998), and then the Akaike information criterion (AIC) was generated. The Akaike-supported model, the base frequencies, the substitution rates, the proportion of invariable sites, and the gamma distribution shape parameters in AIC were used in phylogenetic analyses. Bayesian analysis was performed to confirm the tree topology for each gene separately using MrBayes 3.1.0 (Huelsenbeck & Ronquist, 2001), running the chain for 1×10^6 generations and setting the 'burn-in' at 1,000. The MCMC (Markov chain Monte Carlo) methods within a Bayesian framework were employed to estimate the posterior probabilities of the phylogenetic trees (Larget & Simon, 1999) using the 50% majority-rule.

2. Results

2.1 *Helicotylenchus microlobus* Perry *in* Perry et al., 1959

2.1.1 Measurements and description

Morphometrics and characteristics of adult specimens were consistent with *H. microlobus* (Table 2; Figure 1). Bodies of females were curved ventrally into a spiral shape when heat-killed. Cuticle had distinct annulation and annuli were 1.5–2.0 µm wide at mid-body. Lip region was hemispherical, continuous from body, with 4–5 annuli. Labial framework prominent and sclerotized. Four incisures were distinct in lateral fields. Two inner incisures fused to form a Y-shaped pattern at the tail end. Lateral field not areolated on the tail. Excretory pore (EP) was 102.6 to 130.5 µm from the anterior end of the body, located at the level of the middle part of the esophageal glands, just posterior to the hemizonid. Hemizonion not seen. Stylet strong, with anteriorly indented or rounded basal knobs, 24.6–27.6 µm long. Orifice of dorsal esophageal gland 12.3–14.1 µm behind stylet base. Metacorpus oval to rounded, well-developed, with a sclerotized

Table 1. Nematode species and accession numbers in the GenBank database

Nematode species	Accession numbers			
	18S (18SnF-18SnR)	28S (D2–D3)	28S (391a-501)	ITS (ITSUniF-Nxy22)
Helicotylenchus microlobus Perry in Perry et al., 1959	PQ180325	PQ182781	PQ180364	
Mesocriconema nebraskense Olson et al,. 2017	PV836695	PV836848	PV836870	
Meloidogyne naasi Franklin, 1965	PV837466		PV837516	PV837500

valve. Esophageal glands were ventrally or ventrolaterally overlapping the intestine. Vulval opening was oval, posteriorly located at 62.6–69.3% of total body length; vagina was almost perpendicular to body axis, about 1/2 vulval body diameter long, vulval lips not protruding, and epiptygma not visible. Reproductive system didelphic with two equally developed outstretched ovaries. Phasmids located from two annuli posterior to four annuli anterior to the anus level. Tail short, 1.1–1.6 anal body diameter long, bearing 8–12 ventral annuli, ending in a pronounced ventral projection (peg), peg conical to digitate, usually rounded terminally, without a mucron. Tail tip without annulation or indistinctly annulated. Male was not observed.

2.1.2 Molecular characterization and phylogenetic relationships

A 1509-bp 18S and a 918-bp 28S (391a-501) rDNA of *H. microlobus* in this study were amplified and sequenced. A blastn search of this species matches well with its corresponding species. From 18S sequence, the studied *H. microlobus* and seven populations of *H. microlobus* (ON117513, ON117514, OR844003, OR844004, OR843993, OR843996, and OR843997) in GenBank yielded 1501, 1500, 1508, 1506, 1506, and 1507 total characters with 99.47, 99.40, 99.93, 99.87, 99.80, 99.80, and 99.87% identity, intraspecific sequence variation for *H. microlobus* was 0.53 (8 nucleotide, nt), 0.60 (9 nt), 0.07

Table 2. Morphometrics of females of *Helicotylenchus microlobus* population in the present study compared to those previously reported

Character	Present study	Subbotin et al. (2015) CA,USA/CD740	Yan et al. (2017)	Mwamula et al.(2020a) Korea/KB-5
n	10	12	15	12
L	728.8 ± 98.9 (574.7–838.2)	739 ± 44.5 (657.0–795.0)	708.5 (600.0–812.0)	732.5 ± 31.1 (680.0–792.9)
a	23.6 ± 1.6 (20.9–25.2)	26.6 ± 1.1 (24.8–28.5)	25.0 (21.4–27.1)	25.6 ± 0.9 (24.4–26.9)
b	5.1 ± 0.6 (4.1–5.9)	5.2 ± 0.2 (4.7–5.5)	5.0 (4.4–5.7)	5.9 ± 0.3 (5.4–6.4)
c	34.8 ± 2.9 (29.7–37.5)	34.8 ± 2.0 (32.1–38.9)	35.4 (30.2–41.7)	37.7 ± 3.1 (31.9–42.9)
c'	1.3 ± 0.2 (1.1–1.6)	1.3 ± 0.1 (1.2–1.5)	1.3 (1.0–1.6)	1.2 ± 0.1 (1.1–1.3)
V	66.0 ± 2.7 (62.6–69.3)	62.6 ± 1.4 (60.4–64.8)	61.8 (60.0–63.7)	60.5 ± 1.1 (58.6–62.0)
Stylet length	26.0 ± 1.1 (24.6–27.6)	28.9 ± 0.7 (27.5–30.0)	27.6 (26.0–29.0)	25.2 ± 0.8 (24.1–26.6)
Stylet conus length	11.1 ± 0.5 (10.3–11.8)	13.2 ± 0.4 (12.5–14.0)	—	11.0 ± 0.6 (10.1–11.9)
DGO	13.3 ± 0.7 (12.3–14.1)	—	—	10.9 ± 0.8 (9.7–12.0)
Pharynx length	142.8 ± 9.5 (133.3–156.5)	140 ± 6.0 (125–145)	142.5 (130.0–152.0)	123.6 ± 3.9 (117.6–128.3)
Lip diameter	5.9 ± 0.5 (5.1–6.3)	6.5 ± 0.2 (6.0–7.0)	—	6.9 ± 0.4 (6.3–7.8)
Lip height	4.5 ± 0.2 (4.2–4.7)	4.2 ± 0.4 (4.0–5.0)	—	4.1 ± 0.3 (3.7–4.6)
Maximum body diameter (vulval body diameter)	30.8 ± 2.8 (25.5–33.3)	27.8 ± 1.2 (26.0– 30.0)	27.3 (25.0–33.0)	28.6 ± 0.8 (27.3–29.6)
Anal body diameter	16.1 ± 1.8 (13.8–18.0)	16.0 ± 1.0 (15.0–17.5)	15.8 (14.0–17.5)	16.0 ± 1.0 (14.6–17.9)
Tail length	21.0 ± 2.9 (15.7–23.8)	21.3 ± 1.7 (19.0–23.0)	20.3 (15.0–25.0)	19.5 ± 1.8 (16.9–23.2)
Excretory pore from anterior end	119.0 ± 11.2 (102.6–130.5)	128 ± 6.3 (114–138)	—	116.5 ± 5.2 (109.3–127.4)
Median bulb (Metacorpus) diameter	13.2 ± 1.8 (10.6–14.9)	—	—	—
Tail annuli number	10.2 ± 0.8 (8.0–12.0)	10.8 ± 1.3 (9–13)	11.6 (10.0–14.0)	9.7 ± 0.5 (9.0–10.0)
MB	56.7 ± 4.5 (48.6–61.4)	—	—	55.5 ± 2.2 (51.4–58.6)
Ventral peg length	5.0 ± 1.6 (3.3–7.4)	—	—	3.9 ± 0.9 (2.2–5.3)

All measurements are in μm and in the format: mean ± s.d. (Range).
Note: *n* = number of specimens on which measurements are based; *L* = overall body length; *V* = % distance of vulva from anterior relative to body length; *a* = body length / greatest body diameter; *b* = body length/pharynx length; *c* = body length/tail length; *c'* = tail length/tail diameter at anus; DGO = dorsal gland opening; MB = % distance of center of the middle esophageal bulb from anterior relative to esophageal length.

(1 nt), 0.13 (2 nt), 0.20 (3 nt), 0.20 (3 nt), and 0.13% (2 nt), respectively.

From the 28S (391a-501) sequence, alignment of the studied *H. microlobus* with other eleven populations of *H. microlobus* (KM506793, KM506796, KM506798, KM506800, MG770482, MN764323, MZ707554, ON014759, ON261356, OR844021, and PQ044580) in GenBank revealed 99.83, 99.83, 99.48, 99.30, 99.44, 99.45, 99.18, 99.50, 99.59, 99.45, 98.86% identity, respectively. Compared to these eleven populations, there were respective nucleotide differences of 0.17 (1/575), 0.17 (1/575), 0.52 (3/575), 0.70 (4/575), 0.56 (4/719), 0.55 (4/727), 0.82 (6/734), 0.50 (3/727), 0.41 (3/734), 0.55 (4/727), 1.14% (8/704) in the overlapping region of the partial LSU sequences.

Phylogenetic analyses of the partial 18S and 28S (391a-501) were performed to examine the relationships among the most common species from this study and related species from Genbank. The dendrogram inferred from 18S rDNA sequences (Figure 2) using *Tylenchorhynchus annulatus* (Cassidy, 1930) Golden, 1971 as an outgroup demonstrates: *i*) the 40 selected species/populations of *Helicotylenchus* together with the present study *H. microlobus* population are in a monophyletic clade with 100% posterior probability (pp); *ii*) the species/populations of *Helicotylenchus* are distinctly grouped into two highly supported (100% pp) clades, one clade includes *H. microlobus, H. indicus, H. caudatus, H. multicinctus, crenacauda, H. pseudorobustus, H. rotundicauda, H. microcephalus* and *H. asiaticus,* the other contains *H. minzi, H. varicaudatus, H. platyurus, H. digonicus, H. ciceri, H. canadensis, H. scoticus, H. vulgaris, H. digitiformis,* and *H. paracanalis*; (*iii*) the present study *H. microlobus* population is clustered in a highly supported (99% pp) monophyletic clade with the seven selected *H. microlobus* populations (ON117513, ON117514, OR844003, OR844004, OR843993, OR843996, OR843997).

The tree inferred from 28S (391a-501) rDNA sequences (Figure 3) using *Hoplolaimus seinhorsti* Luc, 1958 as an outgroup demonstrates the following: (*i*) the present study *H. microlobus* population and the selected total of 57 species/populations of the genus *Helicotylenchus* are distinctly clustered into three monophyletic clades with respective 85, 85 and 92% pp, the first clade includes *H. microlobus, H. paxillii, H. pseudorobustus, H. leiocephalus, H. digonicus, H. platyurus, H. broadbalkiensis, H. dihystera, H. californicus, H. indicus, H. abunaamai, H. caudatus, H. crenacauda, H. multicinctus, H. erythrinae* and *H. oleae,* the second contains *H. microcephalus, H. asiaticus* and *H. cuspicaudatus,* and the third clade includes *H. minzi, H. vulgaris* and *H. paracanalis; (ii*) the present study *H. microlobus* population is clustered into a highly supported (100% pp) monophyletic clade with the eleven selected *H. microlobus* populations (KM506793, KM506796, KM506798, KM506800, MG770482, MN764323, MZ707554, ON014759, ON261356, OR844021, and PQ044580).

2.2 *Mesocriconema nebraskense* Olson et al., 2017

2.2.1 Measurements and description

Morphometrics and characteristics of adult specimens were consistent with *M. nebraskense* (Table 3; Figure 4). Bodies of females were slightly curved ventrally when heat-killed. The cuticle was distinctly annulated with smooth margins, and annuli 3.2–4.8 µm wide at mid-body. Anastomoses were observed on the body. Lip region bearing two annules that are smaller and narrower than other body annules, continuous with the body. Labial disc elevated surrounding the oral opening. Excretory pore (EP) on the 23–27th annulus from the anterior end, 112.6–138.5 µm from the anterior end. Stylet robust with well-developed basal knobs that possess moderate anterior projections, on the 11–13th annulus from the anterior end. Reproductive system terminating in a straight vagina; postvulval region of the body tapering gradually, ending in a rounded, symmetrical terminus. Vulval opening on the 7–8th annulus from the posterior end. Tail short, on the 4–6th annulus from the posterior end, the anal opening located 2 3 annuli posterior to the vulva. Tail conical, with a single- to multiple-lobed terminus. Male was not observed.

2.2.2 Molecular characterization and phylogenetic relationships

A 1518-bp 18S and a 831-bp 28S (391a-501) rDNA of *Mesocriconema nebraskense* in this study were amplified and sequenced. A blastn search of this species matches well with its corresponding species. From the 18S sequence, the studied *M. nebraskense* and two populations of *M. nebraskense* (KY574844, KY574845) in GenBank yielded 1514 and 1514 total characters with 99.74 and 99.74% identity; intraspecific sequence variation for *M. nebraskense* was 0.26 (4 nt) and 0.26 % (4 nt), respectively.

From the 28S (391a-501) sequence, alignment of the studied *M. nebraskense* with other eight populations of *M. nebraskense* (MN720085, MN720086, MN720087, MN720088, MN720089, MN720090, MH013430, and OR159862) in GenBank revealed 99.06, 99.84, 99.84, 99.34, 99.69, 99.84, 99.85, and 99.84% identity, respectively.

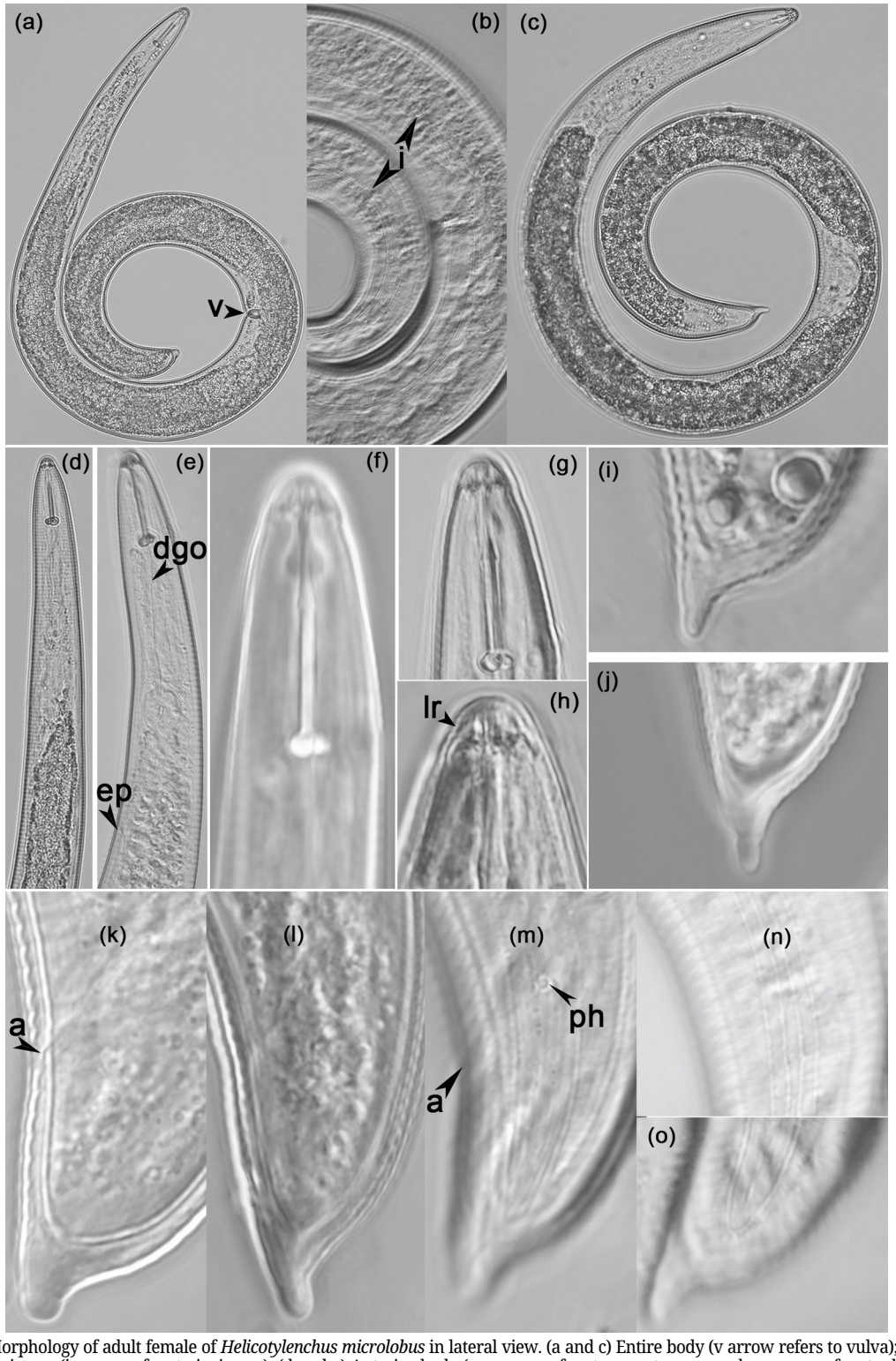


Figure 1. Morphology of adult female of *Helicotylenchus microlobus* in lateral view. (a and c) Entire body (v arrow refers to vulva); (b) Lateral incisures (i arrow refers to incisures); (d and e) Anterior body (ep arrow refers to excretory pore; dgo arrow refers to dorsal gland opening); (f–h) Lip and stylet (lr arrow refers to lip ring); (i–l) Tails (a arrow refers to anus); (m) Phasmid (ph arrow refers to phasmid); (n and o) Lateral incisures at tail (i arrow refers to incisures). (Scale bars: a, c = 50 µm; d, e = 20 µm; b, f–n = 10 µm).

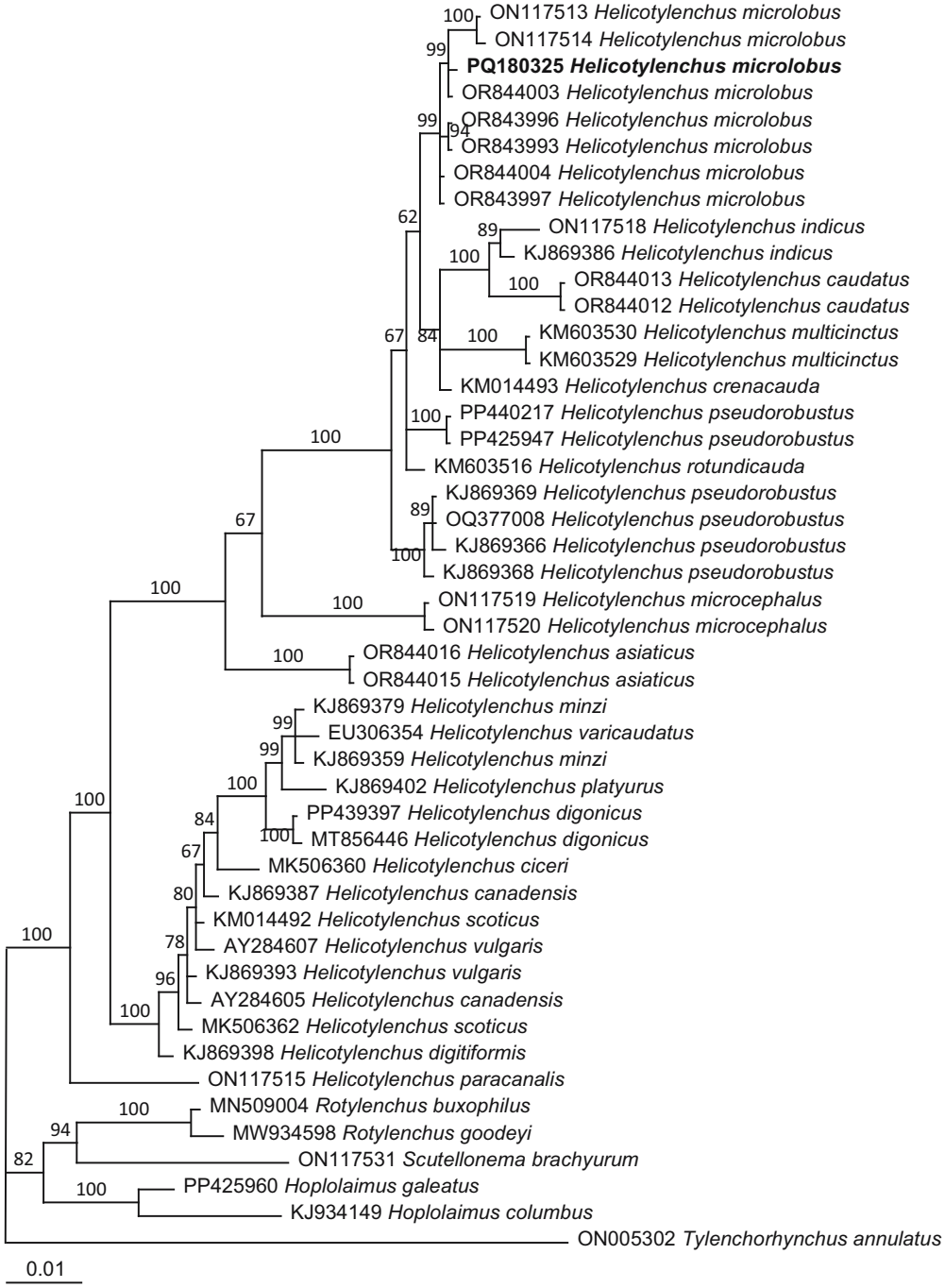


Figure 2. The 10001st Bayesian tree inferred from 18S (18SnF-18SnR) under the TrN + I + G model (lnL = 5160.3901; freqA = 0.2421; freqC = 0.2327; freqG = 0.2760; freqT = 0.2492; R(a) = 1.0000; R(b) = 1.8595; R(c) = 1.0000; R(d) = 1.0000; R(e) = 5.4087; R(f) = 1.0000; Pinvar = 0.6310; Shape = 0.5326). Posterior probability values exceeding 50% are given on appropriate clades. The species in the present study are in bold font.

Compared to these eight populations, there were respective nucleotide differences of 0.94 (6/638), 0.16 (1/642), 0.16 (1/642), 0.66 (4/608), 0.47 (3/641), 0.16 (1/607), 0.15 (1/660) and 0.16% (1/643) in the overlapping region of the partial LSU sequences.

Phylogenetic analyses of the partial 18S and 28S (391a-501) were performed to examine the relationships among the most common species from this study and related species from Genbank. The dendrogram inferred from 18S

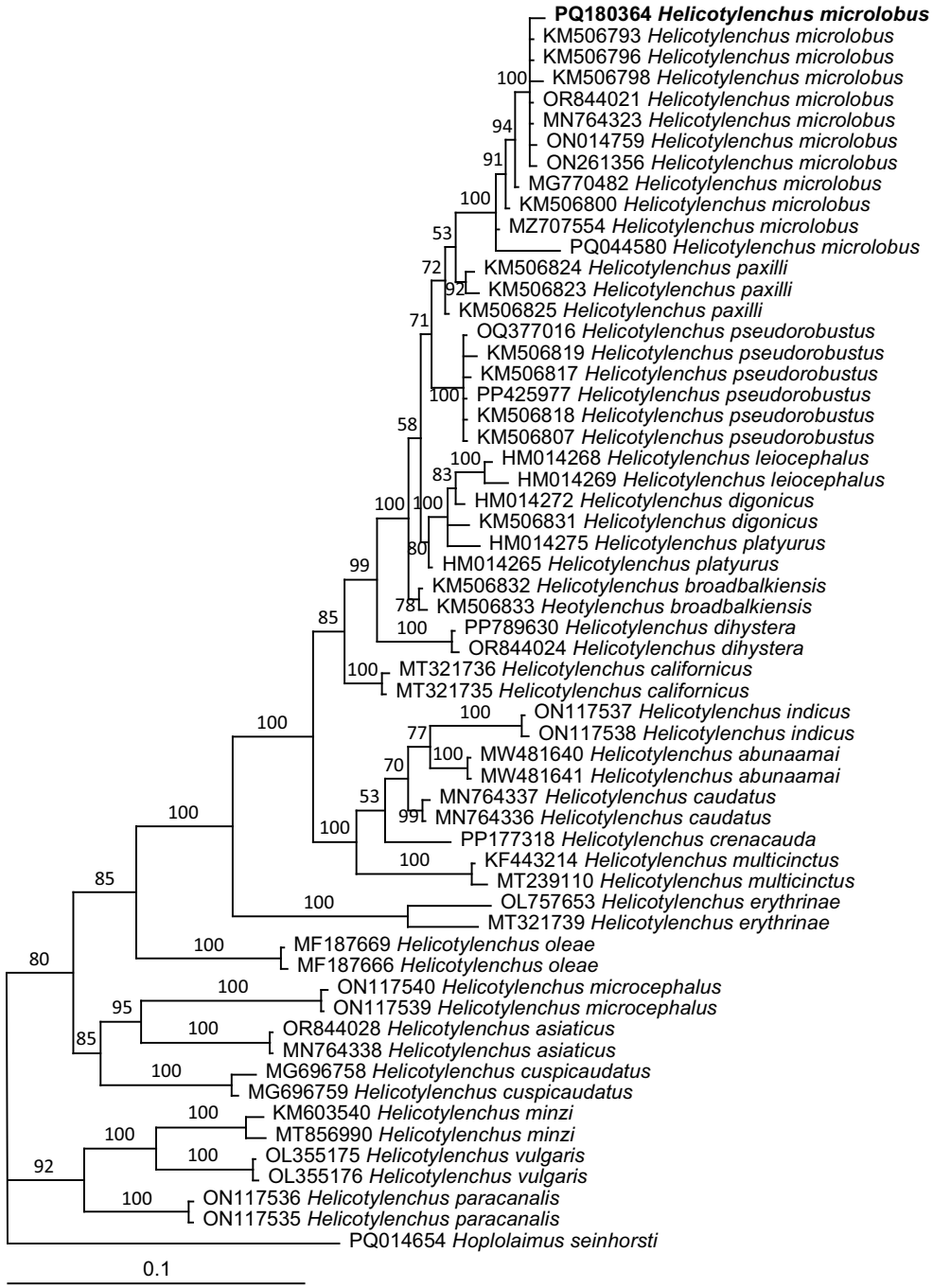


Figure 3. The 10001st Bayesian tree inferred from 28S (391a-501) under the GTR + I + G model (lnL = 4835.0967; freqA = 0.1954; freqC = 0.2466; freqG = 0.3460; freqT = 0.2120; R(a) = 0.3511; R(b) = 1.1538; R(c) = 0.8357; R(d) = 0.3199; R(e) = 3.7157; R(f) = 1.0000; Pinvar = 0.3895; Shape = 0.9532). Posterior probability values exceeding 50% are given on appropriate clades. The species in the present study is in bold font.

rDNA sequences (Figure 5) using *Pratylenchus crenicauda* Winslow, 1958 as an outgroup demonstrates: (*i*) the present study *Mesocriconema nebraskense* population and the selected total of 46 species/populations within 13 genera (*Bakernema, Criconema, Criconemoides, Crossonema, Discocriconemella, Hemicaloosia, Hemicriconemoides, Hemicycliophora, Lobocriconema, Mesocriconema, Neolobocriconema, Ogma* and *paratylenchus*) are distinctly clustered

Table 3. Morphometrics of females of *Mesocriconema nebraskense* population in the present study compared to those previously reported

Character	Present study	Olson et al. (2017)	Yan et al. (2018)	Mwamula et al.(2020b) KP11
n	10	74	10	14
L	521.0 ± 72.3 (440.0–648.0)	508.0 ± 44.5 (393.0–606.0)	546.6 ± 64.0 (425.0–627.0)	549.0 ± 38.4 (505.0–609.0)
a	13.0 ± 2.3 (8.9–15.1)	12.7 ± 1.5 (9.2–15.3)	10.7 ± 1.5 (8.5–13.6)	12.4 ± 0.7 (11.3–13.7)
b	3.4 ± 0.5 (2.8–4.3)	4.4 ± 0.5 (3.6–7.2)	4.4 ± 0.7 (3.9–4.8)	4.5 ± 0.3 (4.1–4.9)
c	19.8 ± 4.4 (15.4–27.3)	—	20.0 ± 2.5 (16.1–25.0)	18.8 ± 1.7 (16.6–21.7)
c'	1.0 ± 0.2 (0.8–1.3)	—	—	1.0 ± 0.1 (0.9–1.2)
V	92.8 ± 1.3 (91.3–94.6)	93.3 ± 0.9 (90.6–96.0)	91.7 ± 0.6 (90.7–92.8)	91.8 ± 0.8 (90.6–92.7)
Stylet length	53.1 ± 2.7 (50.5–56.9)	52.6 ± 2.7 (45.0–59.0)	—	54.2 ± 2.2 (51.2–57.7)
Pharynx length	153.6 ± 22.2 (114.3–182.1)	117.0 ± 10.2 (73.0–135.0)	124.3 ± 8.8 (110.0–140.0)	123.0 ± 4.5 (112.0–129.0)
Maximum body diameter (vulval body diameter)	40.7 ± 6.8 (35.0–53.3)	32.1 ± 2.8 (25.0–39.0)	39.4 ± 3.0 (33.0–40.0)	33.8 ± 1.9 (31.2–36.7)
Anal body diameter	27.3 ± 3.0 (22.6–31.2)	—	29.5 ± 2.8 (25.0–33.0)	28.7 ± 2.0 (25.0–32.0)
Tail length	27.2 ± 6.4 (18.0–37.7)	—	—	29.3 ± 2.3 (25.6–32.1)
Excretory pore from anterior end	125.7 ± 12.2 (112.6–138.5)	—	—	129.0 ± 6.1 (115.0–137.0)
R	92.2 ± 4.4 (87.0–98.0)	102.9 ± 6.1 (84.0–113.0)	105.0 ± 6.0 (98.0–118.0)	96.6 ± 2.5 (94.0–103.0)
R_{st}	11.8 ± 0.8 (11.0–13.0)	—	—	13.3 ± 0.5 (13.0–14.0)
R_{oes}	26.0 ± 1.0 (25.0–27.0)	—	—	24.5 ± 0.9 (23.0–26.0)
R_{ex}	24.8 ± 1.7 (23.0–27.0)	28.0 ± 1.5 (24.0–31.0)	28.3 ± 1.3 (26.0–32.0)	25.7 ± 1.0 (24.0–27.0)
R_{an}	5.0 ± 0.7 (4.0–6.0)	—	5.1 ± 0.3 (5.0–6.0)	5.1 ± 0.3 (5.0–6.0)
R_{v}	7.8 ± 0.4 (7.0–8.0)	7.8 ± 1.0 (6.0–11.0)	9.0 ± 0.7 (8.0–10.0)	7.5 ± 0.9 (6.0–9.0)
R_{van}	2.0 ± 0.1 (2.0–3.0)	—	—	2.1 ± 0.3 (2.0–3.0)

All measurements are in µm and in the format: mean ± s.d. (Range).
Note: *n* = number of specimens on which measurements are based; *L* = overall body length; *V* = % distance of vulva from anterior relative to body length; *a* = body length / greatest body diameter; *b* = body length/pharynx length; *c* = body length/tail length; *c'* = tail length/tail diameter at anus; *R* = ring number of body cuticle; R_{st} = ring number from anterior to base of stylet base; R_{ex} = ring number from anterior to excretory pore; R_{oes} = ring number from anterior to base of esophageal glands; R_{v} = ring number from vulva to tail end; R_{an} = ring number from anus to tail end; R_{van} = ring number between vulva and anus.

into two monophyletic clades with respective 100 and 100% pp, the first clade includes the present study *M. nebraskense* population and 44 species/populations belonging to the genera *Bakernema, Criconema, Criconemoides, Crossonema, Discocriconemella, Hemicaloosia, Hemicriconemoides, Hemicycliophora, Lobocriconema, Mesocriconema, Neolobocriconema,* and *Ogma,* the second contains two species of the genus *Paratylenchus; (ii)* the present study *M. nebraskense* population is grouped into a highly supported (100% pp) monophyletic clade with 15 species/populations within the genus *Mesocriconema*; (*iii*) the present study *M. nebraskense* population is clustered into a highly supported (100% pp) monophyletic clade with other two *M. nebraskense* populations (KY574844 and KY574845) from GenBank.

The tree inferred from 28S (391a-501) rDNA sequences (Figure 6) using *Hemicriconemoides strictathecatus* Esser, 1960 as an outgroup demonstrates: (*i*) the present study *M. nebraskense* population and the selected total of 50 species/populations of the genus *Mesocriconema* are distinctly clustered into two monophyletic clades with respective 100 and 96% pp, the first clade includes the present study *M. nebraskense* population and other eight *M. nebraskense* populations,

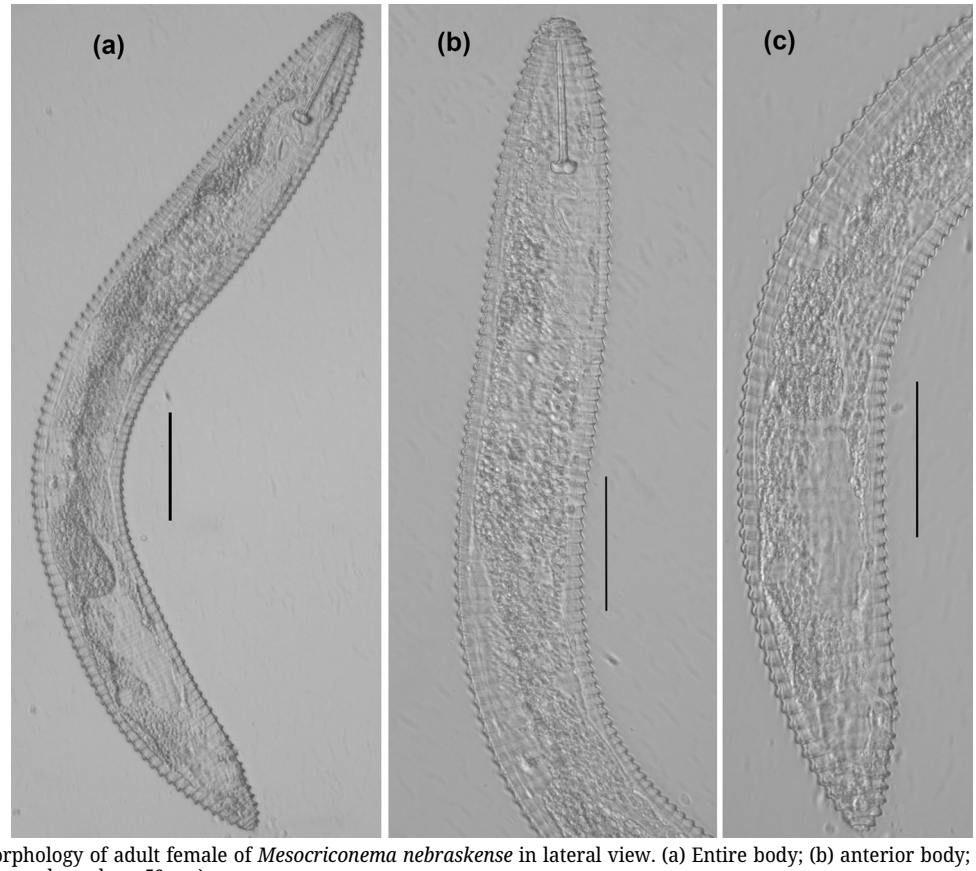


Figure 4. Morphology of adult female of *Mesocriconema nebraskense* in lateral view. (a) Entire body; (b) anterior body; (c) tail. (Scale bars: a, b, and c = 50 µm).

three populations of *M. antipolitanum* (de Guiran) Loof & De Grisse, 1989, one population of *M. basili* (Jairajpuri) Loof & De Grisse, 1989, three populations of *M. curvatum* (Raski) de Grisse & Loof, 1965, five populations of *M. onoense* (Luc) Loof & De Grisse, 1989, six populations of *M. ornatum* (Raski) Loof & De Grisse, 1989, eight populations of *M. xenoplax* and eight *Mesocriconema* sp. populations, and the second clade contains six populations of *M. sphaerocephalum* and one population of *Mesocriconema* sp.*; (ii*) the present study *M. nebraskense* population is clustered into a highly supported (100% pp) monophyletic clade with eight other *M. nebraskense* populations (MN720085, MN720086, MN720087, MN720088, MN720089, MN720090, MH013430 and OR159862) from GenBank, and is sister to *M. xenoplax*.

2.3 *Meloidogyne naasi* Franklin, 1965

2.3.1 Measurements and description

Morphometrics and morphological characteristics of specimens were consistent with *M. naasi* (Table 4; Figure 7). Adult female body was approximately spherical with sharply offset neck: 450.0–700.0 µm in length, 310.0–400.0 µm in greatest diameter. Cuticle clearly annulated on the neck. Excretory pore was located slightly in front of the base of the stylet. Stylet very slender with well-developed knobs tending to slope backwards, 11.0–13.0 µm in length. Metacorpus was large, muscular, with a conspicuous central valve. Gland lobe overlapped the anterior part of the intestine. Intestine together with ovaries filling the swollen part of the body. Eggs were laid within a gelatinous sac outside the female body: 48.0–52.0 µm in length and 23–26 µm in diameter. Perineal pattern on a slight prominence on the spherical body, round to ovoid with a low- to medium-high dorsal arch with large phasmids and a distinct fold over the anus; broken, irregular striae were observed around and between the phasmids.

Body of male curved ventrally at the posterior end when heat-killed. Head scarcely offset from the body. Stylet well-developed with rounded knobs, the anterior pointed part (conus) a little shorter than the posterior part (shaft). Metacorpus fusiform, with central valve plates. Gland lobe lying ventro-laterally along the

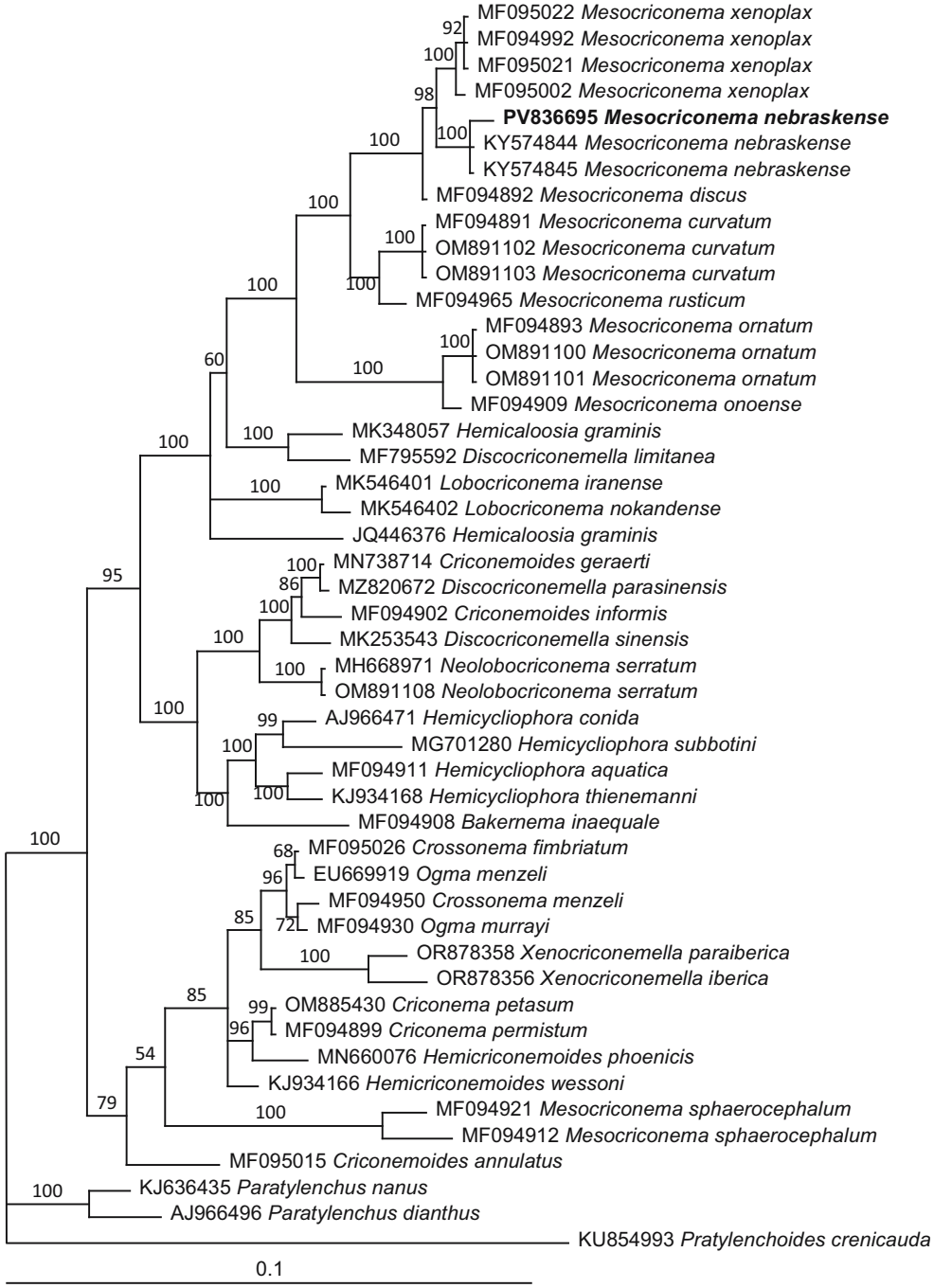


Figure 5. The 10001st Bayesian tree inferred from 18S (18SnF-18SnR) under the GTR + I + G model (lnL = 5450.7681; freqA = 0.2387; freqC = 0.2329; freqG = 0.2919; freqT = 0.2364; R(a) = 1.4422; R(b) = 1.9376; R(c) = 1.1322; R(d) = 0.8133; R(e) = 5.2563; R(f) = 1; Pinvar = 0.6346; Shape = 0.5039). Posterior probability values exceeding 50% are given on appropriate clades. The new species is in bold font.

intestine. Spicules slightly curved ventrally, the distal part tapering to a point, the proximal part broader with thickened margins. Gubernaculum small and saucer-shaped. Tail blunt and very short, with a widely rounded tip.

Body of juvenile slender, slightly curved ventrally when heat-killed. Cuticle with fine annulation. Four incisures in the lateral field. The head is rounded and not offset. The stylet slender and delicate, with rounded and

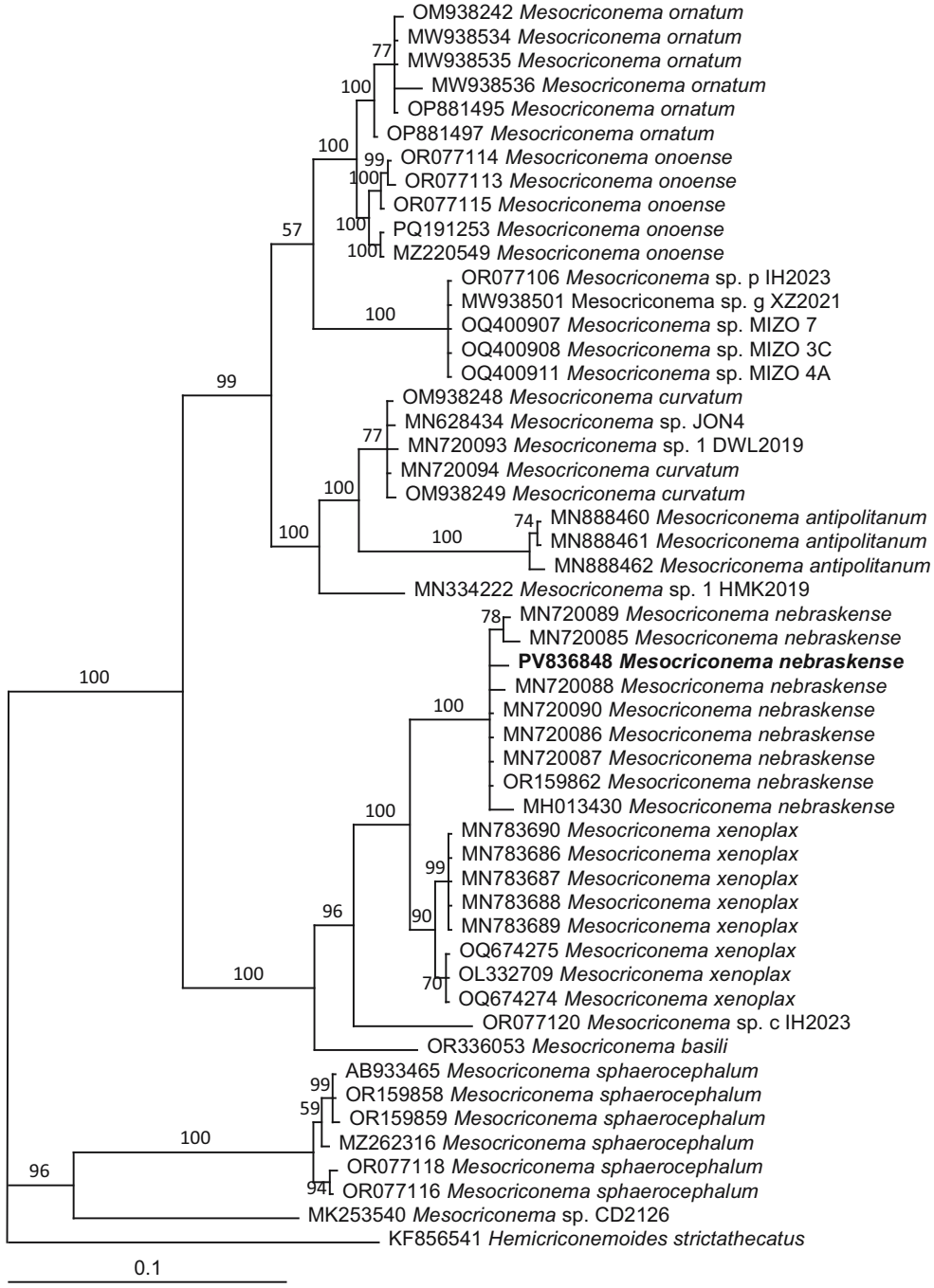


Figure 6. The 10001st Bayesian tree inferred from 28S (391a-501) under the GTR + I + G model (lnL = 3901.4785; freqA = 0.2053; freqC = 0.2451; freqG = 0.3232; freqT = 0.2264; R(a) = 0.7006; R(b) = 1.5219; R(c) = 1.0384; R(d) = 0.5155; R(e) = 4.8247; R(f) = 1; and Pinvar = 0.2547; Shape = 0.6466). Posterior probability values exceeding 50% are given on appropriate clades. The new species is in bold font.

backwardly sloping basal knobs. The dorsal gland duct opening 2.5–3.0 µm behind the stylet knobs. The metacorpus oval, well-developed, with large valve plates in the center. The oesophageal gland lobe ventrally over the intestine. The tail is sharply pointed with a hyaline tail terminus. The tail tip is irregular. The rectum is not swollen. Phasmids not seen.

Table 4. Morphometrics of second-stage juveniles and males of *Meloidogyne naasi* population in the present study compared to those previously reported

Character	Second-stage juveniles (J2)					Males	
	Present study	Zeng et al. (2012a)	Skantar et al. (2023)	Vieira dos Santos et al. (2020)	Franklin (1965)	Present study	Franklin (1965)
n	10	12	30	17	25	10	25
L	459.7 ± 18.1 (443.0–479.0)	431.9 ± 13.4 (414.6–449.6)	427.9 ± 16.7 (390.0–460.0)	457.3 (440.6–478.2)	435.0 (418.0–465.0)	1073.8 ± 110.0 (960.0–1210.0)	1184 (860.0–1316.0)
a	31.6 ± 0.9 (30.6–32.2)	28.8 ± 1.0 (27.5–30.1)	35.6 ± 2.2 (32.2–40.9)	29.6 (27.8–32.6)	28.0 (25.0–32.0)	40.1 ± 0.5 (36.9–40.6)	40 (32.0–48.0)
c	9.0 ± 0.7 (8.2–9.4)	8.0 ± 0.2 (7.9–8.4)	6.1 ± 0.4 (4.9–6.8)	5.5 (5.2–5.8)	6.2	107.9 ± 16.6 (96.0–126.9)	—
c'	5.9 ± 0.3 (5.6–6.1)	6.1 ± 0.2 (5.7–6.2)	—	—	—	0.6 ± 0.1 (0.5–0.7)	—
Stylet length	11.1 ± 0.8 (10.6–12.0)	11.1 ± 0.6 (10.2–11.5)	12.1 ± 0.6 (11.0–13.0)	14.4 (13.6–15.2)	14.0 (13.0–15.0)	16.3 ± 1.3 (15.0–18.0)	18.0 (16.0–19.0)
DGO	2.7 ± 0.3 (2.5–3.0)	—	—	—	3.0 2.0–2.3	2.5 ± 0.6 (2.0–3.0)	3.0 2.0–4.0
Lip diameter	5.5 ± 0.4 (5.1–5.8)	5.4 ± 0.2 (5.2–5.6)	—	—	—	—	—
Lip height	2.4 ± 0.1 (2.3–2.5)	2.3 ± 0.2 (2.1–2.7)	—	—	—	—	—
Metacorpus length	9.5 ± 0.3 (9.2–9.8)	10.0 ± 0.4 (9.3–10.4)	–	—	—	—	—
Metacorpus diameter	7.6 ± 0.7(6.5–8.4)	7.2 ± 0.3(6.8–7.6)	—	—	—	—	—
Maximum body diameter	14.6 ± 0.4 (14.2–15.0)	15.0 ± 0.3 (14.5–15.4)	16.2 (15.0–17.5)	15.5 (14.5–16.7)	15.0 ± 1.0 (14.0–17.5)	27.5 ± 4.0 (24.0–33.0)	30.0 (23.0–34.0)
Anal body diameter	8.7 ± 0.4 (8.4–9.1)	8.9 ± 0.5 (8.4–9.6)	10.3 ± 0.9 (9.0–12.0)	—	11.0 (9.0–13.0)	16.5 ± 1.3 (15.0–18.0)	—
Tail length	51.4 ± 2.7 (48.8–54.2)	53.9 ± 1.9 (52.2–57.1)	70.3 ± 5.0 (62.0–80.0)	82.8 (76.4–89.9)	70.0 (52.0–78.0)	9.5 ± 1.3 (8.0–11.0)	—
Hyaline tail terminus length	21.8 ± 1.4 (20.0–23.2)	22.1 ± 1.8 (20.2–24.4)	21.4 ± 2.2 (17.0–26.0)	26.6 (23.2–32.0)	—	—	—

All measurements are in μm and in the format: mean ± s.d. (Range).
Note: *n* = number of specimens on which measurements are based; *L* = overall body length; *a* = body length / greatest body diameter; *c* = body length/tail length; *c*' = tail length/tail diameter at anus; D*GO* =dorsal gland opening.

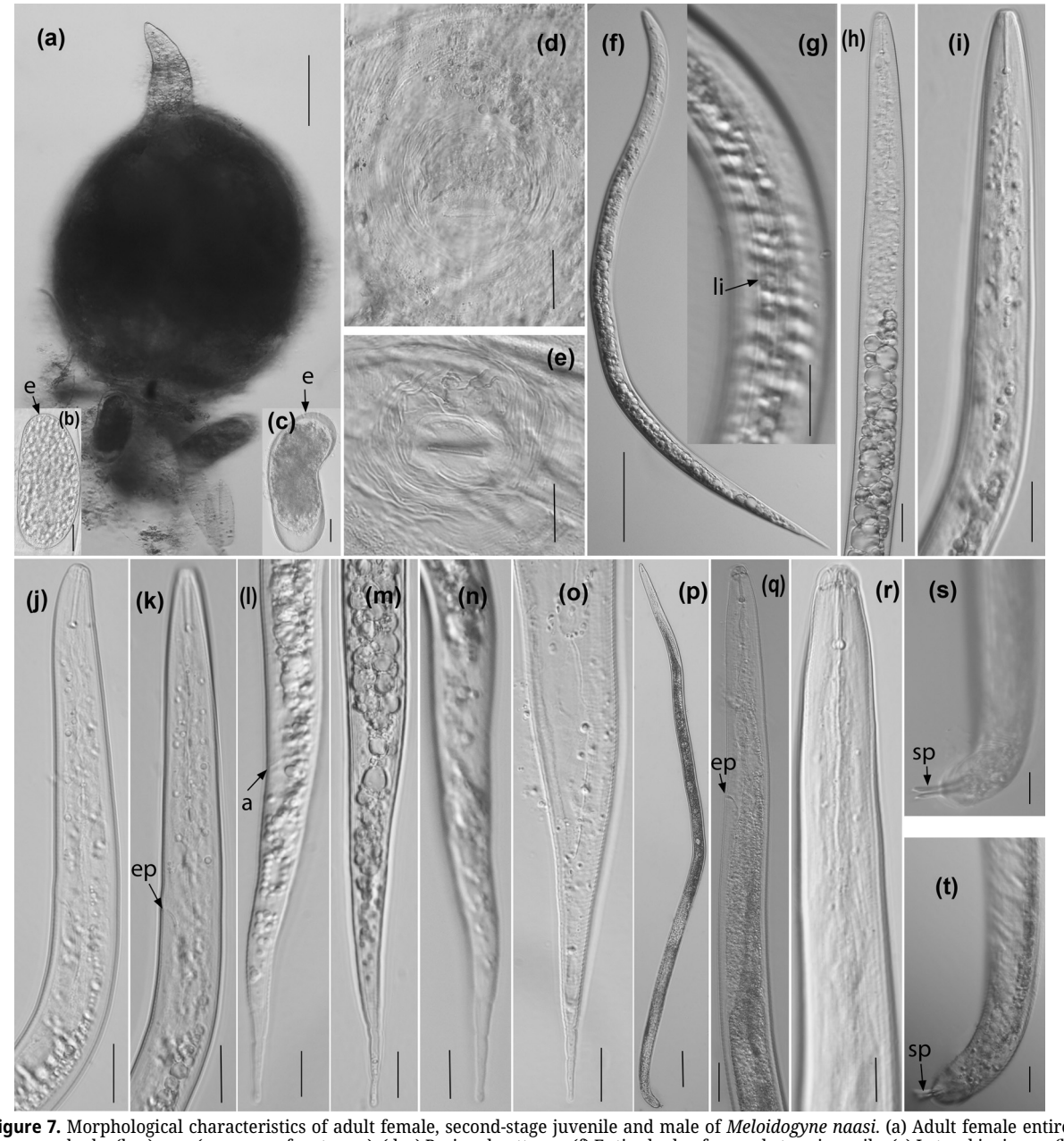


Figure 7. Morphological characteristics of adult female, second-stage juvenile and male of *Meloidogyne naasi*. (a) Adult female entire body; (b, c) eggs (e arrow refers to egg); (d, e) Perineal patterns; (f) Entire body of second-stage juvenile; (g) Lateral incisures (li arrow refers to lateral incisures); (h–k) Anterior body of second-stage juvenile (ep arrow refers to excretory pore); (l–o) Tails of second-stage juvenile (a arrow refers to anus); (p) Male entire body; (q, r) Anterior body of male (ep arrow refers to excretory pore); (s, t) Tails (sp arrow refers to spicule). (Scale bars: a, f, p = 50 µm; d, e, q = 20 µm; b, c, g–o, r–t = 10 µm).

2.3.2 Molecular characterization and phylogenetic relationships

A 1496-bp 18S and an 870-bp 28S (391a-501) rDNA of *Meloidogyne naasi* in this study were amplified and sequenced. A blastn search of this species matches well with its corresponding species. From the 18S sequence, the studied *M. naasi* and three other populations of *M. naasi* (KJ934132, KJ934151, and PP789166) in GenBank each yielded 1496 total characters with 99.80% identity, and each intraspecific sequence variation for *M. naasi* was 0.07 % (1 nt).

From the 28S (391a-501) sequence, alignment of the studied *M. naasi* with other six populations of *M. naasi* (KP901069, MT478999, PP792556, PQ002504, PQ002505, and PQ002506) in GenBank revealed 99.43%, 99.14%, 98.86%, 99.13%, 99.27%, and 99.4527% identity, respectively. Compared to these eleven populations, there were respective nucleotide differences of 0.46 (4/870), 0.86 (6/694), 1.14 (8/704), 0.87 (6/692), 0.73 (5/689), 0.73% (5/689) in the overlapping region of the partial LSU sequences.

Phylogenetic analyses of partial 18S and 28S (391a-501) were performed to examine the relationships among the most common species from this study and related species from GenBank. The dendrogram inferred from 18S rDNA sequences (Figure 8) using *Ditylenchus dipsaci* (Khn, 1857) Filipjev, 1936 and *Merlinius brevidens* (Allen, 1955) Siddiqi, 1970 as outgroups demonstrates the following: (*i*) the 46 selected nematode species/populations together with the present study *M. naasi* population are in a monophyletic clade with 100% pp; (*ii*) the 41 selected *Meloidogyne* species/populations together with the present study *M. naasi* population are in a monophyletic clade with 100% pp; and (*iii*) the present study *M. naasi* population is clustered in a highly supported (100%pp) monophyletic clade with other three *M. naasi* populations (KJ934132, KJ934151, and PP789166) from GenBank.

The tree inferred from 28S (391a-501) rDNA sequences (Figure 9) using *Pratylenchus vulnus* Allen & Jensen, 1951 as an outgroup indicates that (*i*) the present study *M. naasi* population and the selected total of 68 species/populations of the genus *Meloidogyne* are distinctly clustered into two monophyletic clades with respective 100 and 100% pp, the first clade includes *M. aegracyperi, M. arabicida, M. arenaria, M. chitwoodi, M. christiei, M. enterolobii, M. ethiopica, M. exigua, M. fallax, M. floridensis, M. graminicola, M. graminis, M. hapla, M. haplanaria, M. hispanica, M. incognita, M. inonata, M. izalcoensis, M. javanica, M. konaensis, M. lopezi, M. luci, M. marylandi, M. minor, M. morocciensis, M. naasi, M. oryzae, M. paranaensis, M. phaseoli, M. polycephannulata, M. salasi, M. silvestris, M. spartelensis, M. thailandica,* and *M. trifoliophila,* the second contains *M. mali, M. suginamiensis,* and *M. vitis; (ii*) the present study *M. naasi* population is grouped into a highly supported (100% pp) monophyletic clade with six *M. naasi* populations (KP901069, MT478999, PP792556, PQ002504, PQ002505, and PQ002506) from GenBank.

3. Discussion

The paratypes of *H. microlobus* were described by Perry et al. (1959). It has been reported from some countries and regions worldwide, including China (Xia et al., 2022), Korea (Abraham and Dong, 2021), Italy, Spain, Russia (Subbotin et al., 2011), and the USA (Jagdale et al., 2020; Subbotin et al. 2015; Yan et al., 2017). In the United States, it is distributed in over 15 states, including Arizona, California, Florida, Georgia, Idaho, Indiana, Iowa, Maryland, Montana, Nebraska, North Dakota, Oklahoma, Pennsylvania, South Carolina, South Dakota, Tennessee, and Wisconsin (Jagdale et al., 2020; Subbotin et al., 2015; https://maps.eddmaps.org/prevalent/index.cfm? sub = 57607&notitle = 1). *Helicotylenchus microlobus* has been reported infecting soybean (*Glycine max* (L.) Merr.) in North Dakota (Yan et al., 2017), tomato (*Solanum lycopersicum* L.) (Taylor, 1961; Xia et al., 2022), and seashore paspalum (*Paspalum vaginatum* Ws.) in Georgia, USA (Jagdale et al., 2020). The present study population of *H. microlobus* was found in annual bluegrass (*Poa anna* L.) on a golf course in Oakridge Country Club, Utah, USA. To our knowledge, this is the first report of *H. microlobus* from turfgrass in Utah, USA.

The validity of *H. microlobus* as a separate species from *H. pseudorobustus* (Steiner) Golden, 1956 has remained controversial. Some scientists synonymized *H. microlobus* with *H. pseudorobustus* based on morphological similarities between the paratypes of both species (Sher, 1966; Sauer & Winoto, 1975; Fortuner et al., 1984; Firoza & Maqbool, 1994; Brzeski, 1998) and based upon analysis of both quantitative and qualitative characters of these two species (Fortuner et al., 2018), other scientists recognized both *H. microlobus* and *H. pseudorobustus* as valid based upon some morphological differences including areolation (not areolated vs areolated), distal inner lateral incisure fusion pattern (Y-shaped vs M or U-shaped) and phasmid position (consistently at or close to the inner ventral incisures in *H. microlobus*) (Siddiqi, 1972; Subbotin et al., 2015), and based on analysis of molecular data of these two species (Subbotin et al., 2015; Mwamula et al., 2021, 2024). The present study demonstrated that there are morphological differences between *H. microlobus* and *H. pseudorobustus.* Our phylogenetic analysis based upon 18S and 28S rDNA data set showed that the studied *H. microlobus* and *H. pseudorobustus* is clustered in a highly supported (99–100% pp) monophyletic clade with the other *H. microlobus* populations, and is in distinct different monophyletic clade with *H. pseudorobustus* that is grouped into a highly-supported (100% pp) monophyletic clade with the other populations of *H. pseudorobustus* (Figures 2–4), this appears to indicate that *H. microlobus* and *H. pseudorobustus* are not the same species. These results agree with previous studies regarding both *H. microlobus* and *H. pseudorobustus* as valid (Siddiqi, 1972; Subbotin et al., 2015; Mwamula et al., 2021, 2024).

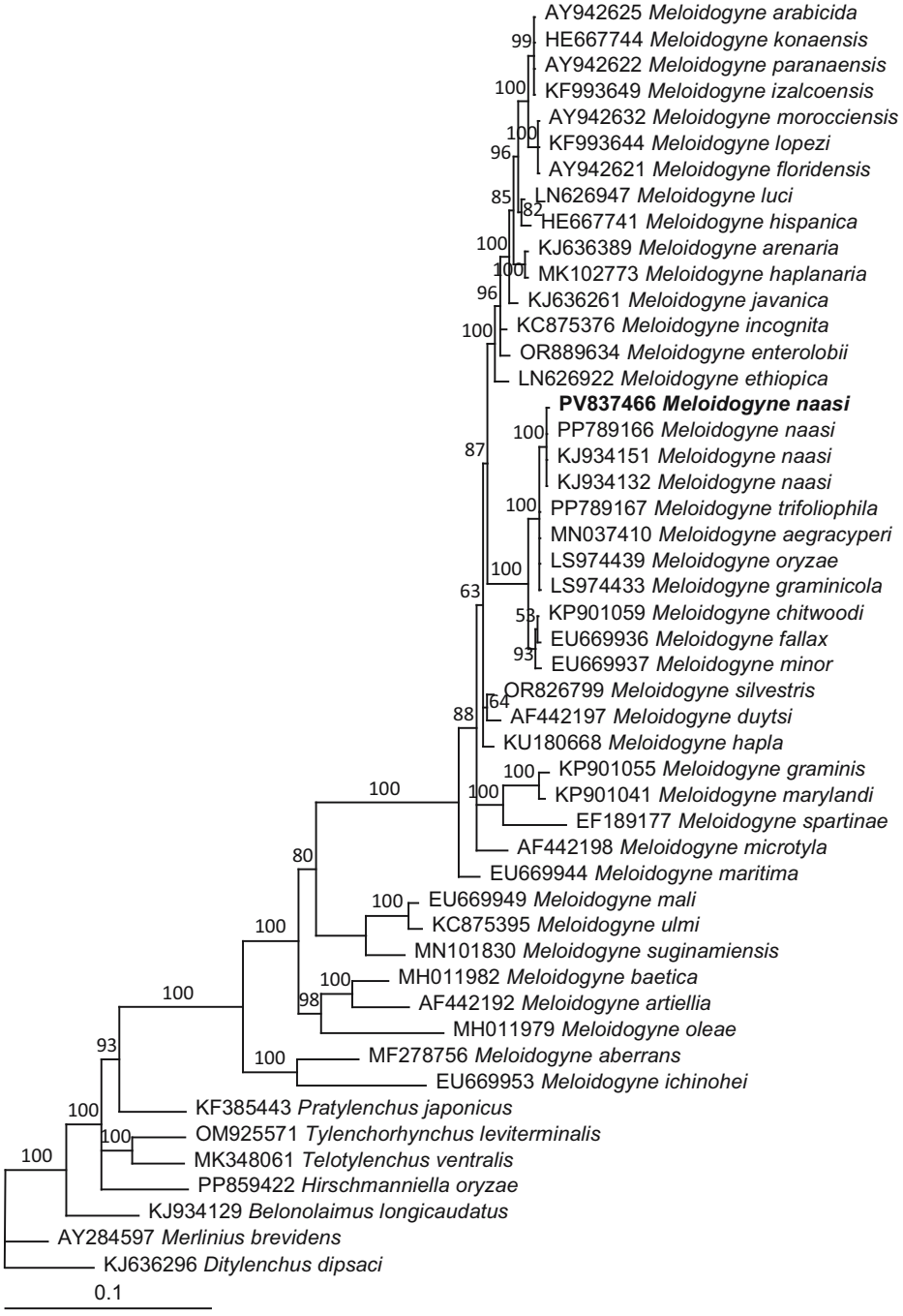


Figure 8. The 10001st Bayesian tree inferred from 18S (18SnF-18SnR) under the GTR + I + G model (lnL = 7594.7705; freqA = 0.2481; freqC = 0.2096; freqG = 0.2740; freqT = 0.2682; R(a) = 1.5624; R(b) = 3.9107; R(c) = 2.0659; R(d) = 0.7165; R(e) = 6.1229; R(f) = 1; Pinvar = 0.5052; Shape = 0.4464). Posterior probability values exceeding 50% are given on appropriate clades. The new species is in bold font.

Thus far *H. asiaticus* Mwamula, Na, Kim, Kim, Han & Lee, 2020, *H. dihystera* (Cobb) Sher, 1961, *H. paxilli* Yuen, 1964 and *H. pseudorobustus* were found on turfgrasses (Crow et al., 2013; Jagdale et al., 2020; Mwamula et al., 2020a; Pang et al., 2011, 2012; Zeng et al, 2012a). However, morphologically the studied *H. microlobus* differs from *H.*

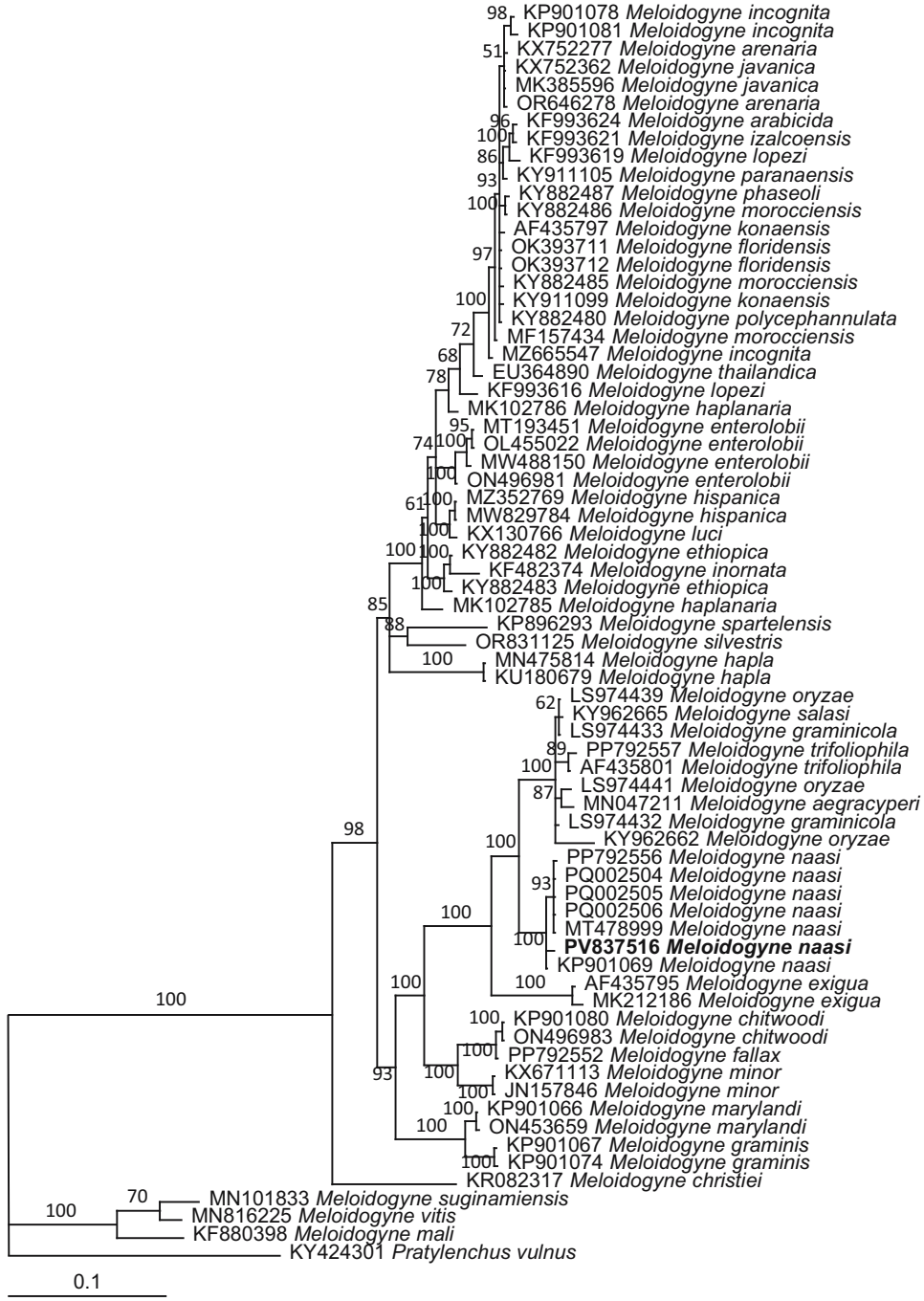


Figure 9. The 10001st Bayesian tree inferred from 28S (301a-501) under the TVM + I + G model (lnL = 6104.6665; freqA = 0.2429; freqC = 0.2162; freqG = 0.1898; freqT = 0.2701; R(a) = 0.2972; R(b) = 0.6776; R(c) = 3.3131; R(d) = 1.6141; R(e) = 3.3131; R(f) = 1; Pinvar = 0.2429; and Shape = 0.7659). Posterior probability values exceeding 50% are given on appropriate clades. The new species is in bold font.

asiaticus by possessing different lateral field (not areolated vs areolated), phasmid position (located at anterior to anus level vs posterior to anus level), and male amount (unknown vs abundant) (Mwamula et al., 2020a), from *H. dihystera* by possessing a lower a (20.9–25.2 vs 27.0–35.0), different tail tip morphology (with pronounced ventral

projection vs slight ventral projection), and phasmid position (2–4 annuli anterior to anus level vs 5–11 annuli anterior to anus level) (Sher, 1966), from *H. paxilli* by possessing a longer DGO (12.3–14.1 vs 7.0–8.0 µm), different lip region morphology (not offset vs offset), phasmid position (located from two annuli posterior to four annuli anterior to anus level vs located from two annuli posterior to 12 annuli anterior to anus level), and tail tip morphology (without mucron vs with) (Yuen, 1964; Subbotin et al., 2015), and from *H. pseudorobustus* by possessing different lateral field (not areolated vs areolated), distal inner lateral incisure fusion pattern (Y-shaped vs M or U-shaped), and phasmid position (consistently at or close to the inner ventral incisures in *H. microlobus*) (Subbotin et al., 2015). Sequence comparative analysis of the 18S rDNA and 28S rDNA (e.g., compared to *H. asiaticus* (OR844030)*, H. dihystera* (MH142614)*, H. paxillin* (KM506825) and *H. pseudorobustus* (KM506807), there were respective nucleotide differences of 10.15 (62/611), 2.98 (18/605), 1.97 (10/507), and 3.16% (16/507) in the overlapping region of the partial 28S rDNA sequences, and molecular phylogenetic inference based upon 18S rDNA and 28S rDNA data set supported that the studied *H. microlobus* is a separate species from *H. asiaticus, H. dihystera, H. paxilli* and *H. pseudorobustus.*

Mesocriconema nebraskense was originally described by Olson et al. (2017) from Spring Creek Prairie, Nebraska, located in the central tallgrass ecoregion of North America. This species has been found in some other states of the USA, including Arkansas, Arizona, Iowa, Illinois, Kansas, Missouri, Minnesota, Nebraska, New Mexico, North Dakota, South Dakota, and Tennessee (Powers et al., 2021; Yan et al., 2018), and in Korea (Mwamula et al., 2020b; Mwamula & Lee, 2021). Several species of the genus *Mesocriconema* Andrássy, 1965, including *M. curvatum, M. xenoplax* Raski, 1952, *M. sphaerocephala* Taylor, 1936, were reported on golf courses in South and North Carolinas (Zeng et al., 2012a,b), New Mexico and Arizona (Yan et al., 2018), and Korea (Mwamula et al., 2020b; Mwamula & Lee, 2021). In this study, *M. nebraskense* was detected from annual bluegrass on a golf course in Utah. This is the first record of *M. nebraskense* from turfgrasses in Utah, USA. So far, it is only known that *M. nebraskense* is associated with grass and corn (Mwamula et al., 2020b; Mwamula a& Lee, 2021; Yan et al., 2018), and its pathogenicity to these plants has not been documented. Clearly, more extensive investigation of this species and research on its impact on the growth of turfgrasses are needed in the future. Molecular phylogenetic analyses revealed that *M. nebraskense* is grouped into a highly supported monophyletic clade with *M. xenoplax* and is sister to *M. xenoplax* (Figures 6–8), which was recently detected from the southern coast of Oregon (Braithwate et al., 2025). However, it differs from *M. xenoplax* by possessing different anastomosis numbers on the female body (1–4 vs rare) and a shorter stylet (45.0–66.0 vs 77.5–85.0 µm) (Olson et al., 2017; Loof & De Grisse, 1989). Compared to these two species, there were nucleotide differences of 14 (1518–1504 = 14) in the overlapping region of the partial 18S SSU sequences, and respective nucleotide differences of 17 (667–650 = 17) and 18 (644–626 = 18) in the overlapping region of 28S LSU D2–D3 and 391a-501 rDNA sequences, supporting the conclusion that these two species are separate species.

Root-knot nematodes (*Meloidogyne* spp.) have been one of the most prevalent species on turfgrasses worldwide (Karssen et al., 2004; Mwamula & Lee, 2021; Oliveira et al., 2018; Vandenbossche et al., 2011; Zeng et al., 2012a). So far, several species of *Meloidogyne* including *M. incognita* (Kofoid & White) Chitwood, 1949 (Ye et al., 2015), *M. graminis* (Sledge & Golden) Whitehead 1968 (Zeng et al., 2012a), *M. graminicola* Golden & Birchfield, 1965 (Mwamula & Lee, 2021), *M. marylandi* Jepson & Golden, 1987 (Oka et al., 2003; Ye et al., 2015), *M. minor* Karssen, Bolk, Van Aelst, Van Den Beld, Kox, Korthals, Molendijk, Zijlstra, Van Hoof & Cook, 2004 (Karssen et al., 2004) and *M. naasi* (Skantar et al., 2023; Zeng et al., 2012a) were reported associated with turfgrasses. *Meloidogyne naasi* was first described by Franklin (1965) from spring-sown barley (*Hordeum vulgare* L.) in Gloucestershire, England and has been reported from other plants including grasses (Bélair et al., 2006; Chaves & Torres, 2000; Crow, 2005; Michell et al., 1973; McClure et al., 2012; Person-Dedryver et al., 1987; Skantar et al., 2023; Vandenbossche et al. 2011; Zeng et al., 2012a,b), oat (*Avena sativa* L.) (Michell et al., 1973), rice (*Oryza sativa* L.) (Michell et al., 1973), sorghum (Michell et al., 1973), sugar beet (*Beta vulgaris* L.) (Mass & Maenhout, 1978), tomato (Dalmasso & Berge, 1978), wheat (*Triticum aestivum* L.) (Roberts et al., 1982), etc. On turfgrasses, *M. naasi* has been reported to be associated with annual bluegrass, creeping bentgrass (*Agrostis stolonifera* L.) (Skantar et al., 2023), bermudagrass (*Cynodon dactylon* (L.) Pers.) and zoysia grass (*Zoysia japonica* Steud.) (Zeng et al., 2012a), in the present study, *M. naasi* was also detected in annual bluegrass at a golf course. So far *M. naasi* was found on grasses in Argentina (Chaves & Torres, 2000), Belgium (Vandenbossche et al., 2011), Canada (Bélair et al., 2006), France (Person-Dedryver et al., 1987), Portugal (dos Santos et al., 2020) and the central western (Michell et al., 1973) and the western (McClure et al., 2012), the southeastern (Zeng et al., 2012), and the southern United States (Crow, 2005). *Meloidogyne naasi* was considered a common species on golf courses distributed from

Southern California to Washington in the coastal or cooler areas of those states in the United States (McClure et al., 2012). *M. naasi* was identified in samples collected from golf course greens in Washington and Utah counties in Utah by sequence analysis using D2–D3 of 28S and ITS rRNA genes (McClure et al., 2012). In the present study, this species was found on a golf course in Davis County, Utah, and documented by combining morphological characterization, morphometrics, and molecular data (characterization and phylogenetic inferences of SSU 18S, LSU 28S, and ITS sequences). However, detailed information on its distribution and pathogenicity to turfgrasses is still lacking. Clearly more extensive sampling for this species and further research on its host range and impact on growth of turfgrasses are needed.

Species identification of spiral (*Helicotylenchus* spp.), ring (*Mesocriconema* spp.) and root-knot (*Meloidogyne* spp.) nematodes is challenging given very small and minute morphological differences. Molecular markers have often been employed for taxonomic identification and phylogenetic analyses in different species of these nematodes (McClure et al., 2012; Olson et al., 2017; Subbotin et al., 2011; Ye et al., 2015; Zeng et al., 2015). Some studies have demonstrated that the 28S region of nuclear rDNA provides useful genetic markers for the accurate identification of sibling species and morphospecies (Rybarczyk-Mydłowska et al., 2019; Subbotin et al., 2011, 2015). During the present study, two pairs of primers (D2A-D3B and 301a-501) were tested for amplification of 28S rDNA for *H. microlobus*, *Mesocriconema nebraskense,* and *Meloidogyne naasi*; the results showed that the primers 301a-501worked well for these three species, and the primers D2A-D3B worked well for *H. microlobus* and *Mesocriconema nebraskense.* The analysis based on molecular data from the 28S rDNA gene sequence amplified using both D2A-D3B and 301a-501 has been shown to provide good phylogenetic resolution. This revealed the utility of the 28S sequence amplified using D2A-D3B or 301a-501 to identify *H. microlobus* and *Mesocriconema nebraskense,* and using 301a-501 to distinguish *Meloidogyne naasi.* These findings highlight the utility of the 28S sequence together with other morphological characters to delineate species boundaries among closely related species.

Acknowledgements

The authors thank Ms Yun Ye for her assistance with extraction, relevant information, and data arrangement of nematodes.

Funding information

Authors state no funding involved.

Author contributions

Y.Z.: Conceptualization, data curation, formal analysis, investigation, methodology, writing-original draft, writing-review and editing; A.V.: Sampling, writing-review and editing; and J.R.: Conceptualization, data curation, methodology, supervision, writing-review and editing.

Conflict of interest statement

The authors state no conflict of interest.

References

Bélair, G., Simard, L., and Eisenback, J. D. 2006. First report of the barley root-knot nematode *Meloidogyne naasi* infecting annual bluegrass on a golf course in Quebec, Canada. Plant Disease 90:1109.

Braithwate, E., Starchvick, R. J., Kwalewski, A. R., Temple, T. N., Baker, H., Kitner, M., Peetz, A. B., Zasada, I. A., and Rivedal, H. M. 2025. A community analysis of plant-parasitic nematodes on coastal Oregon golf coure putting greens. Plant Disease 109:2416–2425.

Brzeski, M. W. 1998. Nematodes of Tylenchina in Poland and temperate Europe, Museum and Institute of Zoology, Polish Academy of Sciences, Warsaw.

Cassidy, G. H. 1930. Nematode associated with sugar cane in Hawaii. Hawaiian Planters Records 34:379–387.

Chaves, E., and Torres, M. S. 2000. Nematode fauna associated with golf courses in the south-eastern region of the Buenos Aires province. Nematofauna asociada a campos de golf en el sudeste de la provincia de Buenos Aires. Revista de la Facultad de Agronomía (Universidad de Buenos Aires) 20:379–386.

Crow, W. 2005. Plant parasitic nematodes on golf course turf. Pest Management 12:10–15.

Crow, W. T., Habteweld, A., and Bean, T. 2020. Mist chamber extraction for improved diagnosis of *Meloidogyne* spp. from golf course bermudagrass. Journal of Nematology 52:e2020–96.

Crow, W. T., Luc, J. E., Sekora, N. S., Pang, W. 2013. Interaction between *Belonolaimus longicaudatus* and *Helicotylenchus pseudorobustus* on bermudagrass and seashore paspalum hosts. Journal of Nematology 45:17–20.

Dalmasso, A. and Berge, J. B. 1978. Molecular polymorphism and phylogenetic relationships in some *Meloidogyne* spp.: Application to the taxonomy of *Meloidogyne*. Journal of Nematology 10:323–332.

Firoza, K., and Maqbool, M. A. 1994. A diagnostic compendium of the genus *Helicotylenchus* Steiner, 1945 (Nematoda: Hoplolaimidae). Pakistan Journal of Nematology 12:11–50.

Fortuner, R., Louis, P. Y., and Geniet, D. 2018. On the morphometric identity of populations of *Helicotylenchus pseudorobustus* (Steiner, 1914) Golden, 1956 (Tylenchida: Hoplolaimidae). Nematology 20:423–439.

Fortuner, R., Maggenti, A. R., and Whittaker, L. M. 1984. Morphometrical variability in *Helicotylenchus* Steiner, 1945. 4: Study of field populations of *H. pseudorobustus* and related species. Revue de Nématologie 7:121–135.

Franklin, M. T. 1965. A root-knot nematode, *Meloidogyne naasi* n. sp., on field crops in England and Wales. Nematologica 11:79–86.

Golden, A. M. 1970. Classification of the genera and higher categories of the order Tylenchida (Nematoda). In: Zuckerman, B. M., Mai, W. F. and Rohde, R. A. (Eds.), *Plant Parasitic Nematodes. Volume 1. Morphology, Anatomy, Taxonomy and Ecology*. Academic Press Inc., New York and London, pp. 191–232.

Hooper, D. J. 1970. Handling, fixing, staining and mounting nematodes. In *Laboratory Methods For Work With Plant And Soil Nematodes*. 5th edition, pp. 39–54. London: Her Majesty's Stationery Office.

Huelsenbeck, J. P., and Ronquist, F. 2001. MR BAYES: Bayesian inference of phylogenetic trees. Bioinformatics 17:1754–755.

Jagdale, G. B., Ali, M. E., Waliullah, S., Hajihassani, A., Martin, K., and Martinez-Espinoza, A. D. 2020. First report of the spiral nematode *Helicotylenchus microlobus* infecting *Paspalum vaginatum*, seashore paspalum turfgrass, in Georgia, USA. Plant Disease 104:2739.

Jenkins, W. R. 1964. A rapid centrifugal-flotation technique for separating nematodes from soil. Plant Disease Reporter 48:692.

Kanzaki, N., and Futai, K. 2002. A PCR primer set for determination of phylogenetic relationships of *Bursaphelenchus* species within the *xylophilus*-group. Nematology 4:35–41.

Karssen, G., Bolk, R. J., Vanaelst, A. C., Vanden Beld, I., Kox, L.F.F., Korthals, G., Molendijk, L., Zijlstra, C., Van Hoof, R., and Cook, R. 2004. Description of *Meloidogyne minor* n. sp. (Nematoda: Meloidogynidae), a root-knot nematode associated with yellow patch disease in golf courses. Nematology 6:59–72.

Larget, B., and Simon, D. L. 1999. Markov chain Monte Carlo algorithms for the Bayesian analysis of phylogenetic trees. Molecular Biology and Evolution 16:750–759.

Loof, P. A. A., and De Grisse, A. 1989. Taxonomic and nomenclatorial observations on the genus *Criconemella* De Grisse & Loof, 1965. Sensu Luc & Raski, 1981. Mededelingen Faculteit Landbouwwetenschappen Rijksuniversiteit Gent 54:53–74.

Maas, P. W. T. and Maenhout, C. A. A. A. 1978. The grass root-knot nematode (*Meloidogyne naasi*) on sugar beet. Gewasbescherming 9:159–166.

McClure, M. A., Nischwitz, C., Skantar, A. M., Schmitt, M. E., and Subbotin, S. A. 2012. Root-knot nematodes in golf course greens of the western United States. Plant Disease 96:635–647.

Michell, R. E., Malek, R. B., Taylor, D. P., and Edwards, D. I. 1973. Races of the barley root-knot nematode, *Meloidogyne naasi*. I. Characterization by host preference. Journal of Nematology 5:41–44.

Mwamula, A. O., and Lee, D. W. 2021. Occurrence of plant-parasitic nematodes of turfgrass in Korea. The Plant Pathology Journal 37:446–454.

Mwamula, A. O., Kabir, Md. F., Lee, G., Choi, I. H., Kim, Y. H., Bae, E. J., and Lee, D. W. 2020b. Morphological characterisation and molecular phylogeny of several species of Criconematina (Nematoda: Tylenchida) associated with turfgrass in Korea, as inferred from ribosomal and mitochondrial DNA. Nematology 22:939–956.

Mwamula, A. O., Kwon, O. G., Kwon, C., Kim, Y. S., Kim, Y. H., and Lee, D. W. 2024. A revision of the phylogeny of *Helicotylenchus* Steiner, 1945 (Tylenchida: Hoplolaimidae) as inferred from ribosomal and mitochondrial DNA. The Plant Pathology Journal 40:171–191.

Mwamula, A. O., Lee, G., Kim, Y. H., Kim, Y. H., Lee, K. S., and Lee, D. W. 2021. Molecular phylogeny of several species of Hoplolaimina (Nematoda: Tylenchida) associated with turfgrass in Korea, with comments on their morphology. Nematology 23:559–576.

Mwamula, A. O., Na, H., Kim, Y. H., Kim, Y. H., Han, G. and Lee, D. W. 2020a. Characterization of a new spiral nematode, *Helicotylenchus asiaticus* n. sp., and three known species from Korea; with comments on the validity of *Helicotylenchus microlobus* Perry *in* Perry, Darling and Thorne, 1959. European Journal of Plant Pathology 157:565–581.

Nadler, S. A., Bolotin, E., and Stock, S. P. 2006. Phylogenetic relationships of *Steinernema* Travassos, 1927 (Nematoda: Cephalobina: Steinernematidae) based on nuclear, mitochondrial, and morphological data. Systematic Parasitology 63:161–181.

Nunn, G. B. 1992. Nematode molecular evolution. Ph.D. dissertation. University of Nottingham, UK.

Oka, Y., Karssen, G., and Mor, M. 2003. Identification, host range and infection process of *Meloidogyne marylandi* from turf grass in Israel. Nematology 5:727–734.

Oliveira, S. A., Oliveira, C. M. G., Maleita, C. M. N., Silva, M. F. A., Abrantes, I. M. O., and Wilcken, S. R. S. 2018. First report of *Meloidogyne graminis* on golf courses turf-grass in Brazil. PLoS One 13: e0192397.

Olson M., Harris T., Higgins R., Mullin P., Powers K., Olson S., and Powers T. O. 2017. Species delimitation and description of *Mesocriconema nebraskense* n. sp. (Nematoda: Criconematidae), a morphologically cryptic, parthenogenetic species from North American grasslands. Journal of Nematology 49: 42–66.

Palomares-Rius, J. E., Cantalapiedra-Navarrete, C., Archidona-Yuste, A., Vovlas, N., Tzortzakakis, E. A., and Castillo, P. 2018. Molecular and morphological characterization of the spiral nematode *Helicotylenchus oleae* Inserra, Vovlas and Golden, 1979 (Nematoda: Hoplolaimidae) in the Mediterranean Basin. European Journal of Plant Pathology 150:881–891.

Pang, W., Luc, J. E., Crow, W. T., Kenworthy, K. E., Giblin-Davis, R. M., McSorley, R., and Kruse, J. K. 2012. Field responses of bermudagrass and seashore paspalum to sting and spiral nematodes. Journal of Nematology 43:201–208.

Pang, W., Luc, J. E., Crow, W. T., Kenworthy, K. E., McSorley, R., Kruse, J. K., and Giblin-Davis, R. M. 2011. Responses of seashore paspalum cultivars to sting and spiral nematodes. Crop Science 51:2864–2867.

Perry, V. G., Darling, H. M., and Thorne, G. 1959. Anatomy, taxonomy and control of certain spiral nematodes attacking blue grass in Wisconsin. Research Bulletin, University of Wisconsin 207:1–24.

Person-Dedryver, F., Gueye, P. S., and Boulch, M. F. 1987. Grasses as hosts of *Meloidogyne naasi* Franklin: II. Study of nematode populations and their effects on yield of three varieties. Nematologica 33:72–82.

Posada, D., and Crandall, K. A. 1998. Modeltest: testing the model of DNA substitution. Bioinformatics 14:817–818.

Powers, T. O., Harris, T. S., Higgins, R. S., Mullin, P. G., and Powers, K. S. 2021. Nematode biodiversity assessments need vouchered databases: A BOLD reference library for plant-parasitic nematodes in the superfamily Criconematoidea. Genome, 64:232–241.

Roberts, P. A., Van Gundy, S. D., and Waines, J. G. 1982. Reaction of wild and domesticated *Triticum* and *Aegilops* species to root-knot nematodes (*Meloidogyne*). Nematologica 28: 182–191.

Rybarczyk-Mydłowska, K., Dmowska, E., and Kowalewska, K. 2019. Phylogenetic studies on three *Helicotylenchus* species based on 28S rDNA and mtCOI sequence data. Journal of Nematology 51:1–17.

Sánchez-Arce, O., Palacios-Espinosa, A., Carillo-Fasio, J., Hernandez-Montiel, L. G., Hernández-Rubio, J. S., and Romero, M. 2021. Diversity and distribution of plant-parasitic nematodes on golf courses in localities of Baja California Sur, Mexico. Revista de la Facultad de Agronomía La Univ. Del Zulia 38:651–660.

Sauer, M. R., and Winoto, R. 1975. The genus *Helicotylenchus* Steiner, 1945 in West Malaysia. Nematologica 21:341–350.

Sher, S. A. 1966. Revision of the Hoplolaiminae (Nematoda). VI. *Helicotylenchus* Steiner, 1945. Nematologica 12:1–56.

Shokoohi, E., Marais, M., Mashela, P. W., and Divsalar, N. 2021. Morphological and molecular variations within *Helicotylenchus vulgaris*. Biologia 76:549–563.

Siddiqi, M. R. 1972. On the genus *Helicotylenchus* Steiner, 1945 (Nematoda: Tylenchida), with descriptions of nine new species. Nematologica 18:74–91.

Siddiqi, M. R., Mukherjee, B., and Dasgupta, M. K. 1982. *Tylenchorhynchus microconus*'n. sp., *T. crassicaudatus leviterminalis*'n. subsp. and *T. coffeae* Siddiqi and Bask, 1959 (Nematoda: Tylenchida). Systematic Parasitology 4: 257–262.

Skantar, A. M., Handoo, Z. A., Kantor, M. R., and Hult, M. N. 2023. First report of barley root-knot nematode, *Meloidogyne naasi* from turfgrass in Idaho, with multigene molecular characterization. Journal of Nematology 55: e20232024.

Subbotin, S. A., Inserra, R. N., Marais, M., Mullin, P., Powers, T., Roberts, P. A., Van den Berg, E., Yeates, G. W., and Baldwin, J. G. 2011. Diversity and phylogenetic relationships within the spiral nematodes of Helicotylenchus Steiner, 1945 (Tylenchida: Hoplolaimidae) as inferred from analysis of the D2-D3 expansion segments of 28S rRNA gene sequences. Nematology 13: 333–345.

Subbotin, S. A., Vovlas, N., Yeates, G. W., Hallmann, J., Kiewnick, S., Chizhov, V. N., Manzanilla-Lopez, R. H., Inserra, R. N., and Castillo, P. 2015. Morphological and molecular characterization of *Helicotylenchus*

pseudorobustus (Steiner, 1914) Golden, 1956 and related species (Tylenchida: Hoplolaimidae) with a phylogeny of the genus. Nematology 17:27–52.

Tamura, K., Peterson, D., Peterson, N., Stecher, G., Nei, M., and Kumar, S. 2011. MEGA5: Molecular evolutionary genetic analysis using maximum likelihood, evolutionary distance, and maximum parsimony methods. Molecular Biology and Evolution 28:2731–2739.

Taylor, D. P. 1961. Biology and host-parasite relationships of the spiral nematode, *Helicotylenchus microlobus.* Proceedings of the Helminthological Society of Washington 28:60–66.

Vandenbossche, B., Viaene, N., De Sutter, N., Maes, M., Kareeen, G., and Bert, W. 2011. Diversity and incidence of plant-parasitic nematodes in Belgian turf grass. Nematology 13:245–256.

Vieira dos Santos, M. C., Almeida, M. T. M., and Cost, S. R. 2020. First report of *Meloidogyne naasi* parasitizing turfgrass in Portugal. Journal of Nematology 52:1–4. DOI:doi: 10.21307/jofnem-2020-088

Williams, B. D., Schrank, B., Huynh, C., Shownkeen, R., and Waterston, R. H. 1992. A genetic mapping system in *Caenorhabditis elegans* based on polymorphic sequence-tagged sites. Genetics 131:609–624.

Xia, Y., Li, J., Xu, F., Lei, B., Li, H., Wang, K., and Li, Y. 2022. Identification and a culture method for a *Helicotylenchus microlobus* from tomato in China. BMC Zoology 7:42.

Yan, G., Plaisance, A., Huang, D., and Handoo, Z. A. 2017. First report of the spiral nematode *Helicotylenchus microlobus* infecting soybean in North Dakota. Journal of Nematology 49:1.

Yan, G., Plaisance, A., Huang, D., Baidoo, R., Ransom, J. K., and Handoo, Z. A. 2018. First report of the ring nematode *Mesocriconema nebraskense* from a corn field in North Dakota. Journal of Nematology 50:531–532.

Ye, W. 1996. Applying Microsoft Works spread sheet in statistics for morphometric data of nematode identification. Afro-Asian Journal of Nematology 6:203–211.

Ye, W., Giblin-Davis, R. M., Braasch, H., Morris, K., and Thomas, W. K. 2007. Phylogenetic relationships among *Bursaphelenchus* species (Nematoda: Parasitaphelenchidae) inferred from nuclear ribosomal and mitochondrial DNA sequence data. Molecular Phylogenetics and Evolution 43:1185–1197.

Ye, W., Robbins, R. T., and Kirkpatrick, T. 2019. Molecular characterization of root-knot nematodes (*Meloidogyne* spp.) from Arkansas, USA. Scientific Reports 9:15680.

Ye, W., Zeng, Y., and Kerns, J. 2015. Molecular characterization and diagnosis of root-knot nematodes (*Meloidogyne* spp.) from turfgrasses in North Carolina, USA. PLoS One 10:e0143556.

Yu, Q., Potter, J. W., and Gilby, G. 1998. Plant-parasitic nematodes associated with turfgrass in golf courses in southern Ontario. Canadian Journal of Plant Pathology 20:304–307.

Yuen, P. H. 1964. Four new species of *Helicotylenchus* Steiner (Hoplolaiminae: Tylenchida) and a redescription of *H. canadensis* Waseem, 1961. Nematologica 10:373–387.

Zameleh, F. M., Karegar, A., Ghaderi, R., and Hesar, A. M. 2020. Morphological and molecular characterisation of *Helicotylenchus ciceri* n. sp. and *H. scoticus* Boag and Jairajpuri, 1985 (Nematoda: Hoplolaimidae) from Iran. Nematology 22:611–626.

Zeng, Y., Chen, X., Ni, Y., Zhao, C., Kerns, J., Tredway, L., and Roberts, J. 2022. Morphological and Molecular Characterization of Prevalent Plant-Parasitic Nematodes from Turfgrasses in Guangdong, China. Horticulturae 8:611.

Zeng, Y., Ye, W., Kerns, J., Tredway, L., Martin, S., and Martin, M. 2015. Molecular characterization and phylogenetic relationships of plant-parasitic nematodes associated with turfgrasses in North and South Carolina, United States. Plant Disease 99:982–993.

Zeng, Y., Ye, W., Tredway, L., Martin, S. and Martin, M. 2012a. Taxonomy and morphology of plant-parasitic nematodes associated with turfgrasses in North and South Carolina, USA. Zootaxa 3452:1–46.

Zeng, Y., Ye, W., Martin, S., Martin, M., and Tredway, L. 2012b. Diversity and occurrence of nematodes associated with turfgrasses in North and South Carolina, USA. Journal of Nematology 44:345–355.